



**HAL**  
open science

## Reinterpretation of the enigmatic Ordovician genus **Bolboporites (Echinodermata).**

Emeric Gillet, Bertrand Lefebvre, Véronique Gardien, Emilie Steimetz,  
Christophe Durllet, Frédéric Marin

► **To cite this version:**

Emeric Gillet, Bertrand Lefebvre, Véronique Gardien, Emilie Steimetz, Christophe Durllet, et al.. Reinterpretation of the enigmatic Ordovician genus Bolboporites (Echinodermata).. *Zoosymposia*, 2019, 15 (1), pp.44-70. 10.11646/zoosymposia.15.1.7 . hal-02333918

**HAL Id: hal-02333918**

**<https://hal.science/hal-02333918>**

Submitted on 13 Nov 2020

**HAL** is a multi-disciplinary open access archive for the deposit and dissemination of scientific research documents, whether they are published or not. The documents may come from teaching and research institutions in France or abroad, or from public or private research centers.

L'archive ouverte pluridisciplinaire **HAL**, est destinée au dépôt et à la diffusion de documents scientifiques de niveau recherche, publiés ou non, émanant des établissements d'enseignement et de recherche français ou étrangers, des laboratoires publics ou privés.

1 **Reinterpretation of the Enigmatic Ordovician Genus *Bolboporites***  
2 **(Echinodermata)**

3

4 EMERIC GILLET<sup>1</sup>, BERTRAND LEFEBVRE<sup>1,3</sup>, VERONIQUE GARDIEN<sup>1</sup>, EMILIE  
5 STEIMETZ<sup>2</sup>, CHRISTOPHE DURLET<sup>2</sup> & FREDERIC MARIN<sup>2</sup>

6

7 <sup>1</sup> *Université de Lyon, UCBL, ENSL, CNRS, UMR 5276 LGL-TPE, 2 rue Raphaël Dubois, F-*  
8 *69622 Villeurbanne, France*

9 <sup>2</sup> *Université de Bourgogne - Franche Comté, CNRS, UMR 6282 Biogéosciences, 6 boulevard*  
10 *Gabriel, F-2100 Dijon, France*

11 <sup>3</sup> *Corresponding author, E-mail: bertrand.lefebvre@univ-lyon1.fr*

12

13 **Abstract**

14 *Bolboporites* is an enigmatic Ordovician cone-shaped fossil, the precise nature and systematic affinities of  
15 which have been controversial over almost two centuries. For the first time, a wide range of techniques  
16 (CT-scan, SEM, cathodoluminescence, XPL, UV epifluorescence, EBSD, FT-IR and XRF spectrometry)  
17 were applied to well-preserved specimens of *Bolboporites* from Norway and Russia. Our main finding  
18 confirms its echinoderm affinities, as shown by its stereomic microstructure and by the first definitive  
19 evidence of its monocrystalline nature. Each cone consists in a single, microporous calcitic crystal with a  
20 narrow longitudinal internal canal. These results are combined with all previous data on *Bolboporites* to  
21 critically discuss five alternative interpretations of this fossil, namely theca, basal cone, spine, columnal,  
22 and holdfast, respectively. The most parsimonious scenario considers *Bolboporites* as an isolated spine,  
23 which was articulated in life by a short biserial appendage to the body wall of an unknown echinoderm,  
24 possibly of echinozoan affinities.

25

26

27 **Introduction**

28

29 The endoskeleton of echinoderms is a complex, multi-element structure typically consisting  
30 of several thousands of individual plates bound together in life by soft tissues (including  
31 collagen fibres) and each consisting of monocrystalline calcite. Taphonomic experiments  
32 suggest that collagen decays relatively soon after the death of the organism (within days or  
33 weeks), thus leading to the collapse and rapid disarticulation of the skeleton into isolated  
34 plates and/or sometimes, more resistant modules (Donovan 1991; Brett *et al.* 1997). The  
35 assignment of an isolated skeletal element to the phylum Echinodermata is generally  
36 straightforward and relies on the presence of a typical three-dimensional meshlike

37 microstructure, the stereom (Smith 1980a; Kouchinsky *et al.* 2012). However, both the  
38 potential diagenetic alteration of the stereom and the high morphological disparity of skeletal  
39 elements within a same individual (e.g., columnals, holdfast, spines) make it often difficult to  
40 identify, and sometimes interpret, such isolated plates, especially in the case of Palaeozoic  
41 taxa that have no current representatives (Berg-Madsen 1986; Pisera 1994; Zamora *et al.*  
42 2013).

43 The situation is further complicated by the existence of numerous morphological  
44 convergences in echinoderms. For example, Palaeozoic deposits have yielded several  
45 relatively similar-looking, small, bowl- to cone-shaped structures (e.g., *Cymbionites*  
46 Whitehouse, 1941; *Oryctoconus* Colchen & Ubaghs, 1969; *Peridionites* Whitehouse, 1941;  
47 *Timorocidaris* Wanner, 1920). Their nature and precise taxonomic assignment (at class level)  
48 has often been strongly debated (Bather 1920; Gislén 1947; Schmidt 1951; Ubaghs 1968b,  
49 1978a; Smith 1982; Alvaro & Colchen 2002; Seilacher & MacClintock 2005; Zamora *et al.*  
50 2009). However, most of them are now convincingly interpreted either as pelmatozoan  
51 holdfasts (e.g., *Oryctoconus*; Alvaro & Colchen 2002; Seilacher & MacClintock 2005;  
52 Zamora *et al.* 2009), highly specialized columnals (e.g., Sumrall *et al.* 1997), basal thecal  
53 plates of eocrinoids (e.g., *Cymbionites*, *Peridionites*; Smith 1982) or highly derived crinoid  
54 calices made of few, tightly sutured ('fused') plates (e.g., *Timorocidaris*; Bather 1920;  
55 Ubaghs 1978a).

56 On the other hand, the interpretation of some other isolated echinoderm elements remains  
57 problematic and controversial. This is the case for the enigmatic Ordovician genus  
58 *Bolboporites* Pander, 1830, which corresponds to centimetric cone-shaped calcitic fossils,  
59 with a typical honeycomb-like ornamentation on their external lateral surface (Fig. 1B). The  
60 base of the cone is smooth, flat to strongly convex, and bears two adjoining, shallow  
61 depressions (Fig. 1A). Within this depressed area, a tiny orifice (Fig. 1A) opens into a narrow,  
62 longitudinal canal extending internally towards the apex of the cone (Yakovlev 1921;  
63 Yeltysheva 1955; Clark & Hofmann 1961; Rozhnov & Kushlina 1994a).

64 *Bolboporites* is particularly widespread and abundant in Baltica, where it is recorded from  
65 the Dapingian to the Darriwilian (e.g., Estonia, Russia; Pander 1830; Eichwald 1857; Bassler  
66 1911; Yakovlev 1921; Yeltysheva 1955; Smith 1988; Kushlina, 1995, 2007; Federov 2003;  
67 Rozhnov & Kushlina 1994a; Rozhnov 2005) and locally to the Sandbian (e.g., Norway,  
68 Sweden; Kjerulf 1865; Lindström 1883; Kushlina 1995). This genus also occurs in the late  
69 Darriwilian of Laurentia (e.g., New York, Quebec, Virginia; Hall 1847; Billings 1859; Logan  
70 *et al.* 1863; Brainerd & Seely 1888, 1896; Miller 1889; Brainerd 1891; Ami 1896; White

71 1896; Ruedemann 1901; Raymond 1905, 1906, 1913; Bassler 1915; Twenhofel 1938; Butts  
72 1940; Clark 1944, 1952; Oxley & Kay 1959; Clark & Hofmann 1961; Shaw & Bolton 2011).  
73 *Bolboporites* was also reported in the Tramore Limestone Formation of Ireland (Avalonia;  
74 Reed 1899), in deposits recently assigned to the late Darriwilian (Wyse Jackson *et al.* 2002).

75 This genus was originally described based on material from the Saint-Petersburg area  
76 (Russia) by Pander (1830), who considered that it was closely related to *Dactylopora*  
77 Lamarck, 1816 (see also Milne-Edwards & Haime 1851), then interpreted either as a  
78 bryozoan or as a foraminiferan, and now assigned to the algae (Dasycladales; see, e.g., Génot  
79 & Granier 2011). In North America, the first specimens of *Bolboporites* were reported in  
80 Quebec by Hall (1847), who described them as *Chaetetes* Fischer von Waldheim, 1829 (i.e., a  
81 genus of hypercalcified sponges; see Stanton *et al.* 2016). This Canadian material was later  
82 reidentified as *Bolboporites* by Billings (1859), who interpreted it as a zoophyte. Affinities  
83 with anthozoans, and in particular with tabulate corals close to *Favosites* Lamarck, 1816,  
84 were frequently suggested for *Bolboporites* (Bronn 1849; Bronn 1851–1856; Eichwald 1857,  
85 1860; Fromental 1861; Kjerulf 1865; Zittel 1879; Ruedemann 1901; Butts 1940). Yakovlev  
86 (1921) made the first sections through specimens of *Bolboporites*, thus demonstrating the  
87 presence of the longitudinal axial canal and internal growth lines. Based on these new  
88 observations, he concluded that *Bolboporites* was a highly derived stromatoporoid.

89 Possible echinoderm affinities for *Bolboporites* were first questioned by Logan *et al.*  
90 (1863), Quenstedt (1881) and Lindström (1883), based on the observation of stereom  
91 microstructure. Miller (1889) interpreted Russian specimens of *Bolboporites* as probable  
92 echinoderms, but North American ones as corals. With few exceptions (see above), the  
93 assignment of *Bolboporites* to echinoderms was finally accepted by most authors in the late  
94 19<sup>th</sup> century. However, its nature and precise taxonomic affinities remained largely debated  
95 and enigmatic (Jaekel 1899; Bassler 1911; Régnell 1956, 1982; Smith 1988). Quenstedt  
96 (1881) was the first to point out that the morphology of *Bolboporites* was similar to that of  
97 isolated asteroid or echinoid spines. This interpretation was followed by several authors, who  
98 interpreted *Bolboporites* as probable spines belonging to various groups of echinoderms:  
99 asteroids (Lindström 1883; Yeltysheva 1955; Régnell 1956); echinoids (Wanner 1920); or  
100 ‘cystoids’ close to *Palaeocystites tenuiradiatus* (Hall, 1847) (Clarke & Hoffman 1961).

101 An alternative hypothesis was proposed by Ami (1896), who considered that *Bolboporites*  
102 was not an isolated spine, but the internal mould of the theca of an unknown ‘cystoid’.  
103 Following this interpretation, von Wöhrmann (*in* Jaekel 1899) suggested that *Bolboporites*  
104 was possibly the internal mould of a cheirocrinid rhombiferan (see also Régnell 1956). This

105 interpretation of *Bolboporites* as corresponding to the body capsule (theca) of a ‘cystoid’ was  
106 further elaborated by Rozhnov & Kushlina (1994a, b), based on the observation of two sets of  
107 small skeletal elements articulated into the two depressions on the convex surface of some  
108 well-preserved specimens. These two series of plates were interpreted as elements of a single  
109 feeding appendage (brachiole), which was inserting onto the convex (oral) surface of a highly  
110 derived eocrinoid (Rozhnov & Kushlina 1994a, b; Kushlina 1995, 2006, 2007; Rozhnov  
111 2005, 2009). In this interpretation, the central longitudinal canal corresponds to the stem,  
112 which was entirely surrounded by massive, fused thecal plates.

113 Recently, the examination by one of us (BL) of numerous individuals of *Coelosphaeridium*  
114 Roemer, 1885 (a genus of Ordovician calcareous green algae; see Kato *et al.* 1987; Spjeldnaes  
115 & Nitecki 1990; Baarli 2008) from the Sandbian of Norway showed remarkable similarities in  
116 size, morphology and external ornamentation with co-occurring specimens of *Bolboporites*  
117 from the same levels and localities. This observation thus questioned the echinoderm  
118 affinities of *Bolboporites* (Lefebvre 2014, 2017). As a consequence, the aims of this paper  
119 were to apply for the first time a wide range of techniques (e.g., cathodoluminescence, CT-  
120 scan, FT-IR analyses, SEM, EBSD) on well-preserved specimens of *Bolboporites*, so as to  
121 test their putative echinoderm affinities and, if confirmed, to discuss the nature of  
122 *Bolboporites* (isolated skeletal element *vs.* body capsule), as well as its systematic position  
123 within the phylum Echinodermata.

124

125

## 126 **Material and Methods**

127

128 **Material.** This study is based on 28 specimens of *Bolboporites* from Norway and Russia. The  
129 ten Norwegian specimens were selected within the abundant material of *Bolboporites* sp.  
130 (about 100 individuals) belonging to the collections of the Paleontologisk Museum, Oslo  
131 (acronym: PMO). All Norwegian specimens of *Bolboporites* were originally collected in 1975  
132 by J.F. Bockelie in bioclastic deposits of the Fossum Formation (Sandbian), at Gravastranda,  
133 Herøya (Skien-Langesund area, Norway). These levels are generally interpreted as relatively  
134 shallow-water deposits yielding abundant and diverse benthic assemblages regularly  
135 smothered by storm deposits (Bockelie 1981; Owen *et al.* 1990). The fauna is dominated by  
136 brachiopods, bryozoans, echinoderms (caryocystitid and cheirocrinid rhombiferans,  
137 eocrinoids, crinoids, edriasteroids) and trilobites, associated to rare cephalopods and  
138 graptolites (Bockelie 1981; Owen *et al.* 1990).

139 Eighteen individuals of *Bolboporites mitralis* Pander, 1830, from Russia were made  
140 available for this study by S.V. Rozhnov, who donated them to the palaeontological  
141 collections of Lyon 1 University (acronym: UCBL). This material was collected on the banks  
142 of the Lynna river (Saint-Petersburg area) in the upper member (BII $\gamma$ , Frizy Limestone) of the  
143 Volkhov Formation. This ~3 m thick stratigraphic unit is dated as early Darriwilian, based on  
144 the occurrence of both conodonts typical of the *Baltoniodus norrlandicus* Zone and trilobites  
145 characteristic of the Scandinavian *Megistaspis simon* Zone (Federov 2003; Dronov 2005).  
146 The upper member of the Volkhov Formation consists predominantly of nodular, glauconitic  
147 limestones, with several intercalated levels of shales. The bioclastic limestones are generally  
148 interpreted as storm-generated deposits, in a shallow-water, temperate setting (Dronov 2005).  
149 In these levels, faunal assemblages are dominated by brachiopods, ostracods and isolated  
150 pelmatozoan remains, associated to bryozoans, conulariids, graptolites and trilobites (Federov  
151 2003).

152

153 **Methods.** As Norwegian specimens are preserved as mouldic impressions in the rock, their  
154 original external aspect was revealed by making latex casts, which were coated with  
155 ammonium chloride (NH<sub>4</sub>Cl) for observation and photographic purposes. External  
156 morphological features of *Bolboporites* sp. from Norway were observed at Lyon 1 University,  
157 with a Zeiss SteREO Discovery.V8 stereomicroscope binocular and captured with a Zeiss  
158 AxioCam MRc5 digital camera.

159 In contrast to the Norwegian material, the Russian specimens are preserved as three-  
160 dimensional fossils, thus allowing the application of a wider range of techniques of  
161 observation and analyses. Several Russian specimens were embedded in hydrophilic acrylic  
162 resin of low viscosity (LR white resin), allowing longitudinal and transverse sections with a  
163 Leica SP 1600 saw microtome. Other Russian specimens were set in epoxy resin and cut to  
164 make polished thin sections with a thickness of 30  $\mu$ m and 130  $\mu$ m. Both sections were  
165 observed with a Hitachi TM-100 scanning electron microscope (SEM) at the Université de  
166 Bourgogne, Dijon, so as to document putative internal structures.

167 Thin sections were observed under plane polarized light (PPL), cross-polarized light (XPL)  
168 and epifluorescence UV using a Nikon AZ100 microscope, equipped with a 360 nm exciting  
169 source and a Zeiss AxioCam MRc5 (Université de Bourgogne, Dijon). Polished thin sections  
170 were also observed under cathodoluminescence using a Leica MZ12 binocular microscope  
171 equipped with a Luminoscope ELM-3R device and a Zeiss AxioCam MRc5 camera  
172 (Université de Bourgogne, Dijon). Cathodoluminescence (CL) was successfully applied by

173 Gorzelak & Zamora (2013), so as to reveal the internal stereomic microstructure preserved in  
174 skeletal elements of various Cambrian echinoderms. This technique was usually shown to be  
175 efficient, even in the case of relatively strongly recrystallized specimens.

176 For FT-IR investigations, thin sections were used to extract *in situ* - with the tip of a  
177 scalpel blade - small chips of material from different sampling points located both inside the  
178 fossil and in the surrounding resin. The extracted materials were then reduced into powders  
179 with an agate mini mortar and pestle ( $< 10 \mu\text{m}$ ) and the powder was subsequently analyzed by  
180 Fourier transform infrared (FT-IR) spectroscopy, to identify the different mineralogical  
181 phases, on a ALPHA FT-IR BRUKER device equipped with an ALPHA-P module. Data  
182 acquisition was performed in the  $4000\text{-}500 \text{ cm}^{-1}$  wavenumber range (12 scans at a spectral  
183 resolution of  $4 \text{ cm}^{-1}$ ), in ATR mode (Attenuated Total Reflectance) with a single reflection  
184 diamond crystal adapted to solids. Blank spectra were acquired on resin alone. The qualitative  
185 assignment of absorption bands was performed by comparison with known IR spectra found  
186 in the literature (Jones & Jackson, 1993).

187 The magnesium content of some Russian specimens of *Bolboporites* was checked with a  
188 Bruker S1 Titan spectrometer equipped with a collimated beam and incorporated in a  
189 laboratory console. Every measurement consisted of two successive beam phases of 60  
190 seconds, with energies of 45 kV and 15 kV. This protocol allows measuring equivalent MgO  
191 mass concentrations above 1% in relatively small windows (2 mm in diameter) and directly in  
192 the thicker thin sections.

193 The internal structure of one well-preserved *Bolboporites* was also analyzed with electron  
194 back-scattered diffraction (EBSD), a technique that permits the characterization of complex  
195 polycrystalline materials at nanoscale. In short, it allows measuring and representing - via 2D-  
196 coloured maps and pole figures - the crystallographic orientation of individual nanograins  
197 with respect to each other. This technique, currently used in materials science, is particularly  
198 adapted for calcium carbonate fossil and non-fossil biominerals (Checa *et al.* 2009; Cusack  
199 2016). To this end, an embedded sample was manually mirror-polished on  $0.05 \mu\text{m}$  aluminium  
200 oxide powder and further processed on a vibratory polisher. The sample was fixed on a  
201 sample holder and analyzed on a JEOL JSM 760 F field emission scanning electron  
202 microscope, from which coloured maps were produced, with a step of 250 nm. Measurements  
203 were performed at the periphery of the sample and also in different areas of the central zone  
204 separated from each other by a few millimeters; this allowed detection of potential  
205 crystallographic disorientations at milli-metric scale.

206 Microtomographic observations were performed by using a Bruker CT-scan (Skyscan  
207 1174 model) at the Université de Bourgogne, Dijon (Morphoptics Service), to obtain virtual  
208 cross-sections through some specimens, and also to reconstruct a three-dimensional model of  
209 *Bolboporites*. In recent years, tomography has become a routine technique of imagery, so as  
210 to reveal internal structures in various fossils and, in particular, Palaeozoic echinoderms  
211 (Sutton *et al.* 2005; Rahman & Clausen 2009; Rahman & Zamora 2009; Rahman *et al.* 2010,  
212 2015; Briggs *et al.* 2017). Data acquisition was obtained at 50 kV and 800  $\mu$ A. Two images  
213 per position (number of frames: 2) were obtained, each of them after an exposure time of  
214 2500 ms. The rotation step of the sample was  $0.7^\circ$  and the total acquisition time was 75  
215 minutes.

216 Other individuals of *B. mitralis* were kept intact, so as to explore minute details of their  
217 external morphology. However, in most specimens, the base of the cone and/or the  
218 honeycomb cells on the lateral walls were partly concealed by a thin layer of sedimentary  
219 rock. Consequently, fossils were placed in an ultrasonic cleaner containing a solution of dilute  
220 ethylenediaminetetraacetic acid (EDTA, 1% wt/vol, pH 8) to remove all pieces of surrounding  
221 rock and better expose the external aspect of the specimens. Once cleaned, fossils were rinsed  
222 with water, then with ethanol (C<sub>2</sub>H<sub>5</sub>OH), and finally dried with a hair-dryer. Observation of  
223 the external aspect of the specimens was made using both a Zeiss SteREO Discovery.V8  
224 binocular stereomicroscope, equipped with a Zeiss AxioCam MRc5 digital camera, at  
225 Université Lyon 1, and a Hitachi TM-100 Scanning Electron Microscope (SEM) at the  
226 Université de Bourgogne, Dijon.

227 Finally, three dried specimens of the Recent asteroid *Pentacaster mammilatus* (Audouin,  
228 1826) were examined and prepared for morphological comparison purposes. This material  
229 belongs to the R. Koehler collections, which are part of the zoological collections of Lyon 1  
230 University (acronym: UCBL). The specimens were collected between 1895 and 1930 (precise  
231 date of sampling not reported on labels) from an unknown locality, possibly in the Red Sea or  
232 the western part of the Indian Ocean (Clark & Rowe 1971). Dissection and extraction of some  
233 aboral spines was made with a scalpel. Photographs were made with a Nikon D5000 camera  
234 in the palaeontological collections of Lyon 1 university (CERESE).

235

236

## 237 **Results**

238

239 *Chemical and mineralogical analyses.*



240 The FT-IR spectroscopy performed on transverse sections of *Bolboporites mitralis* included  
241 in LR white resin generated two contrasting sets of infrared spectra, depending on the position  
242 of the sampling points, outside or inside the fossil (Fig. 2). The surrounding LR white resin  
243 produced a characteristic reference IR spectrum (Fig. 2B), while infrared spectra obtained in  
244 sampling points located within the fossils all showed the three absorption bands that are  
245 characteristic of calcite (Fig. 2C-E) at 711-712  $\text{cm}^{-1}$ , 871  $\text{cm}^{-1}$ , and 1395  $\text{cm}^{-1}$ , respectively.  
246 This spectrum is clearly distinct from that of aragonite (not shown), characterized by a  
247 doublet at 700-713  $\text{cm}^{-1}$  and two bands at 858 and 1477  $\text{cm}^{-1}$ , in addition to a sharp one at  
248 1083  $\text{cm}^{-1}$ . No dolomite (identified by absorption bands at 729, 882 and 1441  $\text{cm}^{-1}$ ) was  
249 detected in the central zone, Our data unambiguously showed that the Russian specimens of  
250 *Bolboporites* are entirely made of calcite.

251 A slightly more complex infrared spectrum was observed in sampling points located on  
252 lateral edges of the fossils, with the three absorption bands typical of calcite, but also some  
253 additional minor bands (Fig. 2C, G). Comparison with the 'control' spectrum shows that this  
254 signal corresponds to the combination of both calcite and LR white resin infrared spectra,  
255 resulting from either the irregular external morphology of the body wall (ornamentation  
256 consisting of honeycomb cells), and/or a limited penetration of the resin into micropores and  
257 microfractures of the specimens.

258 Finally, a large absorption band of low amplitude in the 3700-3100  $\text{cm}^{-1}$  range was  
259 observed in one spectrum corresponding to a sampling spot located within the fossil (Fig. 2F).  
260 This signal did not result from any contamination from the resin, but more likely  
261 corresponded to the vibrations of OH bond, suggesting the occurrence of water, putatively in  
262 the form of small fluid inclusions within the calcite.

263 The XRF measurements were made in central and exterior parts of *Bolboporites* sections.  
264 Magnesium was only detected, with MgO values between 1 and 5% (mass concentration), in  
265 most peripheral parts of the skeleton, where analyzed windows encroach the surrounding  
266 sedimentary rock. Close examination of these parts, under SEM and cathodoluminescence  
267 (see below) revealed the presence of small dolomite rhombs, thus driving the Mg content. In  
268 all other parts of the skeleton, Mg was never found, being below the 1% detection limit. Thus,  
269 a low magnesium calcite (LMC) is deduced for their current composition.

270

271 *Microstructures.*

272 Observation of thin sections of *B. mitralis* with a polarizing microscope shows that whole  
273 cones are affected by conjugate cleavage planes (Fig. 3A,C), and have a single and right

274 crystal extinction (Fig 3B), typical of monocrystals. This important result is confirmed by our  
275 investigations using electron backscattered diffraction (EBSD), the outcome of which is  
276 synthesized in Figure 4. When performed on the periphery of the section (Fig. 4A-D), EBSD  
277 mapping shows that the crown interface is constituted of a mixture of micritic grains (2  $\mu\text{m}$  or  
278 less) surrounding sparitic crystals of about tens to more than 100 microns in diameter (Fig.  
279 4B, D) while the upper left corner of the map corresponds to the sample itself, which is  
280 symbolized by one unique colour, and is, consequently, monocrystalline. The EBSD mapping  
281 performed on the central zone of the sample (Fig. 4E-G) shows that the analyzed area is  
282 uniform, with no detectable grain limit. This demonstrates clearly that the structure is  
283 monocrystalline. Interestingly, when maps are produced in different central zones distant  
284 from each other by few millimetres, one notices a slight change of crystallographic  
285 orientation, symbolized by a minor colour change: for example, two zones 1 mm apart (either  
286 in X or Y) show a grain orientation spread of about 0.3 - 0.5°. When the distance is larger  
287 between two analyzed zones (such as 4 mm between Fig. 4F and G), the disorientation is  
288 more important, around 3.73° in the present example. In summary, EBSD mapping confirms  
289 that the calcite that constitutes a specimen of *Bolboporites* is monocrystalline, with a very  
290 minor and gradual crystalline disorientation at millimetric scale, without any detectable grain  
291 limit.

292 Under cathodoluminescence, both transverse and longitudinal sections of *B. mitralis*  
293 revealed the same mottled, orange-to-brown luminescent microstructure (Fig. 5C). Orange  
294 irregular dots and axes are aligned within a browner sealing calcite crystal, forming a CL  
295 pattern usually detected for ancient echinoderm stereoms (e.g., Gorzelak & Zamora 2013).  
296 These orange parts probably represent the former porous stereom that has been secondary  
297 cemented by a syntaxial brown-luminescent cement. Under XPL and PPL, the same stereom-  
298 like microstructure is also detected in some parts of the cones, with the tenuous occurrence of  
299 small dark spots aligned along cleavage planes (Fig. 3C). At a larger scale, the stereom of  
300 *Bolboporites* exhibits a slightly differentiated, darker, narrow peripheral rim in CL (Fig.  
301 5A,B), which probably results either from a diagenetic effect or from a distinct lighter density  
302 of the former microstructure. A similar observation was made on virtual cross-sections of *B.*  
303 *mitralis* obtained by CT-scan, which show a diffuse peripheral rim, consistently lighter than  
304 the darker central part of the fossils (Fig. 6A). In CT-scan imagery, intensity restitution  
305 largely depends on the density of the materials. Consequently, the central part of *Bolboporites*  
306 is currently made of slightly more porous (less dense) skeleton than the periphery. Views by  
307 SEM confirm this deduction, with numerous micropores occurring everywhere in the skeleton,

308 except in its peripheral parts (Fig. 5D), where initial micropores are probably cemented by the  
309 diagenetic brown-luminescent calcite. As shown by cathodoluminescence (Fig. 5A-C), the  
310 internal canal is also cemented by the brown syntaxial calcite.

311 Finally, contrary to these important observations, no structures have been detected within  
312 the cones using UV epifluorescence technique. This is probably due to the absence of  
313 fluorescent organic matter within the stereomic calcite microstructure, in probable relation  
314 with an intense thermal alteration of the organic matter during the burial history of these  
315 Palaeozoic fossils.

316

### 317 *Internal morphological features.*

318 Sections made through specimens of *B. mitralis* confirm previous reports of a narrow, straight  
319 to gently curved, longitudinal canal, extending from the base of the cone towards the apex  
320 (Fig. 5A,C; Yakovlev 1921; Yeltysheva 1955; Clark & Hofmann 1961; Rozhnov & Kushlina  
321 1994a, b). The observation of this longitudinal canal in all specimens, consistently in the same  
322 position, indicates that it corresponds to an original internal structure.

323 In contrast, both transverse and longitudinal sections also demonstrated the presence of  
324 additional, randomly distributed tubulars and incurved holes, opening either on the base or on  
325 the lateral surface of the cone, and penetrating more or less deeply into it (Fig. 5A,B,D).  
326 Optical observations made on thin sections of *B. mitralis* show that these structures are filled  
327 by a wackestone to packstone sediment, containing diverse organic fragments (e.g., shell  
328 debris, echinoderm skeletal elements) and glauconite grains (Fig. 3). In unprepared Russian  
329 specimens (i.e., without ultrasonic cleaning), the nature of this infilling appears to be similar  
330 to the surrounding matrix. Consequently, the random distribution of these holes, their variable  
331 size and depth, as well as their infilling by sedimentary rock, all indicate that they are not  
332 original internal structures, but rather correspond to borings (*Trypanites* isp.) made by  
333 unknown drilling organisms. They are morphologically different from the less penetrative,  
334 though superficially extensive traces already reported on the basal surface of *B. mitralis*  
335 (Kushlina 2006).

336 Apart from the central longitudinal canal and randomly located *Trypanites*-like borings, no  
337 other internal morphological macrostructure was apparent in sections of *B. mitralis*.  
338 Observations made with a polarizing microscope and EBSD show that each specimen of  
339 *Bolboporites* currently consists in a single crystal of calcite (see above). Although the calcite  
340 is recrystallized, the diverse observations of an extensive stereom-like microstructure in all  
341 parts of a sectioned specimen of *Bolboporites* indicates that each cone was originally a

342 microporous, but unique, monocrystal of calcite, with a central canal forming the unique  
343 internal macro-cavity.

344

345 *External morphological features.*

346 Similar external morphological features were observed in all available Norwegian and  
347 Russian specimens of *Bolboporites* (Figs 6B,7,8). These features are in good agreement with  
348 previous descriptions of the external aspect of *Bolboporites* made on specimens from Baltica  
349 (e.g., Yeltysheva 1955; Rozhnov & Kushlina 1994a; Kushlina 1995) and *Laurentia* (e.g.,  
350 Clark & Hofmann 1961).

351 Cells on the lateral walls of the cones typically display rounded to hexagonal outlines (Fig.  
352 8A) and their diameter decreases in the apical direction (Fig. 7A-C). In contrast, cells located  
353 towards the base tend to become larger and more elliptical in shape. Each cell corresponds to  
354 a shallow (less than 1 mm deep), gently concave, smooth depression delimited by raised rims,  
355 thus forming a characteristic honeycomb pattern on the lateral walls of the cone (Figs 7A-C,  
356 8A). After ultrasonic cleaning, SEM observation of Russian specimens revealed the presence  
357 of the typical porous, stereomic microstructure on the external surface of the cells (Fig. 8A).  
358 No specimens express an orifice at the apex of the cones, thus suggesting that their internal  
359 central canal (see above) terminated close to, though not opening at, the apex.

360 The base of the cone is entirely smooth, with the exception of two adjoining circular  
361 depressions (or lunules), each surrounded by a low C-shaped ridge (Figs 7D, 8B). These two  
362 shallow cavities are not in central positions, but more or less displaced laterally (Fig. 7D).  
363 Ultrasonic cleaning of Russian specimens shows that the floor of each depression is gently  
364 concave, entirely smooth and displays a well-preserved, porous stereom microstructure (Fig.  
365 8B). A small orifice occurs at the junction between the two depressions (Figs 7D, 8B). This  
366 opening represents the basal extremity of the internal longitudinal canal (see above). No other  
367 conspicuous external morphological structure (e.g., orifice) could be observed on the basal,  
368 flat to convex surface of the cones.

369

370

## 371 **Discussion**

372

373 Cathodoluminescence, applied here for the first time to *Bolboporites*, confirms previous  
374 reports of the presence of a former stereomic microporous structure in this fossil (e.g., Logan  
375 *et al.* 1863; Lindström 1883; Yeltysheva 1955; Clark & Hofmann 1961). Currently blocked

376 by a diagenetic syntaxial calcite, this microstructure is also detected under SEM and PPL  
377 observations. A second important result is that each specimen of *Bolboporites* corresponds to  
378 a single, formerly porous, monocrystal of calcite. Taken together, these two points provide  
379 definitive evidence for echinoderm affinities. Consequently, overall similarities in shape or  
380 ornamentation with algae (e.g., *Coelosphaeridium*), bryozoans, corals or sponges (e.g.,  
381 stromatoporoids) are merely superficial.

382 The initial calcite stereom is now entirely cemented and recrystallized into an orange-to-  
383 brown luminescent LMC. This low Mg content does not preclude an initial low Mg content  
384 that may have been much higher during the formation of this skeletal element, but modified  
385 (and lowered) during diagenesis. Such a diagenetic pathway is well documented for most  
386 ancient echinoderm stereoms (Gorzalak *et al.* 2016) and for biogenic HMCs in general  
387 (Bischoff *et al.* 1993). Despite this recrystallization, the extensive distribution of stereomic  
388 microstructure everywhere within the cones suggests that, originally, *Bolboporites* did not  
389 contain any internal macro-structure, with the exception of the narrow longitudinal central  
390 canal, which opens within the two lunules, on the base of the cone.

391 These results, combined with all available evidence obtained during this study and/or from  
392 the literature, make it possible to critically evaluate all plausible interpretations concerning  
393 the nature and systematic position of *Bolboporites*. Comparison with other Palaeozoic  
394 echinoderm cone-shaped elements suggests that *Bolboporites* can be interpreted in five  
395 different ways: (1) internal mould or body wall of a blastozoan theca (by analogy with, e.g.,  
396 *Timorocidaris*; Ami 1896; Rozhnov & Kushlina 1994a, b; Kushlina 1995); (2) large  
397 infrabasal cone of the body capsule (calyx or theca) of a stemless pelmatozoan (by  
398 comparison with, e.g., *Cymbionites*); (3) isolated spine or tuberculated plate of an unknown  
399 echinoderm (Quenstedt 1881; Lindström 1883; Wanner 1920; Yeltysheva 1955; Clark &  
400 Hofmann 1961); (4) highly modified columnal of a pelmatozoan; and (5) distal holdfast of a  
401 stemmed echinoderm ('*Oryctoconus* scenario').

402

403 *Bolboporites* as a theca.

404 In this interpretation, *Bolboporites* represents either the internal mould (Ami 1896; von  
405 Wöhrmann *in* Jaekel 1899; Régnell 1956) or the external wall of a blastozoan theca (Rozhnov  
406 & Kushlina 1994a, b; Kushlina 1995, 2006, 2007). In blastozoans, the theca was polyplated  
407 and entirely made of extraxial skeletal elements (i.e., deriving from the pre-metamorphic  
408 larva; David *et al.* 2000; Sprinkle & Guensburg 2001; Nardin *et al.* 2009, 2017). The theca  
409 was bearing all main body orifices (anus, hydropore, mouth) and, when present, various kinds

410 of respiratory structures (e.g., epispores, diplopores, rhombs; Kesling 1968; Sprinkle 1973;  
411 David *et al.* 2000). In life, the theca housed the main body cavity, which contained all internal  
412 organs (e.g., gut; Kesling 1968; Sprinkle 1973; Rahman *et al.* 2015).

413 The interpretation of *Bolboporites* as the internal mould of a blastozoan theca relies on  
414 several arguments: (1) its overall morphology is compatible with the cone-shaped aspect of  
415 the theca of various blastozoans, such as *Rhopalocystis* Ubaghs, 1963; (2) the honeycomb  
416 ornamentation could represent the imprint of thick polygonal thecal plates on the internal  
417 mould; (3) the smooth aspect of the basal surface could result from a more finely-plated oral  
418 surface; and (4) the lunules could correspond to the imprint left by one (or two) body  
419 opening(s). The main problem with this interpretation is that, by definition, the internal mould  
420 of a blastozoan theca corresponds to the infilling of this theca by sedimentary rock. This  
421 implies that the mineralogical composition of the internal mould should be similar to that of  
422 the surrounding rock. However, our results clearly demonstrate that (1) the mineralogical  
423 composition of *Bolboporites* is very distinct from that of the surrounding sedimentary rock;  
424 and (2) this fossil corresponds to a single echinoderm plate (stereom, monocystal of calcite).  
425 Consequently, *Bolboporites* does not represent the internal mould of a blastozoan theca.

426 The second interpretation considers *Bolboporites* as the theca of an eocrinoid blastozoan,  
427 preserved either as an external mould (e.g., Norwegian specimens) or as a recrystallised three-  
428 dimensional fossil (e.g., Russian material). The main argument supporting this interpretation  
429 is the observation of a partially-preserved appendage-like structure inserted onto the lunules,  
430 on the smooth basal surface of some specimens from Russia (Rozhnov & Kushlina 1994a, pl.  
431 6; Kushlina 2007, pl. 1 fig. 3). When present, this structure occurs consistently in the same  
432 location (i.e., perfectly fitting into the lunules), and it always shows a biserial pattern, with  
433 two opposite sets of small, thick, semi-circular skeletal elements. A longitudinal groove is  
434 running on one side of the appendage, along the suture between the two series of opposite  
435 ossicles (see Rozhnov & Kushlina 1994a, pl. 6 fig. 1d). This groove is apparently leading  
436 (proximally) into the small orifice located at the junction between the two lunules.

437 This biserial structure was interpreted by Rozhnov & Kuslina (1994a, b) as a feeding  
438 appendage (brachiole; see also Kushlina 1995, 2006; Rozhnov 2005, 2009). This  
439 identification implies that the groove borne by brachiolar plates probably housed a single ray  
440 of the ambulacral system and that, consequently, the mouth was located at the proximal  
441 extremity of this ray. The mouth would thus correspond to the small orifice located within the  
442 lunule. In their interpretation of *Bolboporites*, Rozhnov & Kushlina (1994a, b) further  
443 suggested that: (1) the internal longitudinal canal of *Bolboporites* was probably homologous

444 to the axial canal (lumen) of a pelmatozoan stem, thus implying that the stem was present, but  
445 entirely encased within the theca; and (2) all organs (e.g., gut) were not located within the  
446 theca, but outside of it, on the smooth surface of the cone.

447 No articulated appendage was preserved in our study material. However, its interpretation  
448 as a brachiole is plausible: in echinoderms, axial (ambulacral) flooring plates typically display  
449 a comparable biserial, zigzag pattern, resulting from their appearance through ontogeny,  
450 alternatively on the left and on the right of a growing ray of the ambulacral system ('ocular  
451 plate rule'; David & Mooi 1996, 1999; Mooi & David 1997, 1998, 2008). This identification  
452 has several implications: (1) the longitudinal groove borne by the flooring plates is an  
453 ambulacral food groove; (2) the orifice located at the proximal extremity of this groove is the  
454 mouth; (3) no ambulacral cover plates are apparently present (or preserved) above this  
455 groove; and (4) *Bolboporites* possessed one single brachiole. The reduction of the number of  
456 feeding appendages is relatively common in Palaeozoic echinoderms. It was documented both  
457 in some crinoids (e.g., *Monobrachiocrinus granulatus* Wanner, 1920; Ausich *et al.* 1999) and  
458 also in various groups of vagile, epibenthic taxa, such as pleurocystitid rhombiferans (Paul  
459 1967; Kesling 1968; Parsley 1970), solutans (Ubaghs 1981; David *et al.* 2000; Lefebvre &  
460 Lerosey-Aubril 2018) and stylophorans (Ubaghs 1968a; David *et al.* 2000; Lefebvre 2003).

461 Our results demonstrate that *Bolboporites* corresponds to a single, massive cone-shaped  
462 echinoderm skeletal element. This observation has two major implications: if *Bolboporites* is  
463 interpreted as the theca of an eocrinoid, then this theca (1) is entirely made of one single plate;  
464 and (2) with the exception of the narrow central canal, it does not contain any internal  
465 structure. Reduction of the number of plates forming the body capsule is a trend described in  
466 various groups of Palaeozoic echinoderms, such as in solutans (e.g., Late Ordovician  
467 belemnocystitids from North America; Parsley & Caster 1965; Caster 1968) or in  
468 stylophorans (e.g., *Jaekelocarpus* Kolata, Frest & Mapes, 1991 from the Pennsylvanian of  
469 Oklahoma; Dominguez *et al.* 2002). Particularly drastic examples of such a reduction in the  
470 number of plates can be documented in the calices of several derived, Late Palaeozoic,  
471 stemless crinoids, all characterized by convergent, similar-looking cone-shaped  
472 morphologies, as, for example, *Agassizocrinus lobatus* Springer, 1926, from the Mississippian  
473 of Kentucky (Ettensohn 1975) or *Edriocrinus sacculus* Hall, 1859, from the Lower Devonian  
474 of New York (Moore 1978; Seilacher & MacClintock 2005; Herbert & Ettensohn 2018). The  
475 stemless Permian crinoid *Timorocidaris* probably represents the most extreme case of  
476 reduction in the number of plates, with its bowl-shaped calyx possibly made of a single

477 skeletal element (Ubaghs 1978a; Hess 1999). Consequently, *Bolboporites* could represent a  
478 case of convergent acquisition of a single plated body capsule in blastozoans.

479 In all echinoderms, including the most extreme crinoid morphologies, the body capsule  
480 always contains an internal cavity housing the viscera. However, our observations show that  
481 *Bolboporites* is a massive skeletal element, without any body cavity. If *Bolboporites* was a  
482 single-plated theca, then its mouth (i.e., the small orifice located within the lunules, at the  
483 proximal extremity of the ambulacral groove) would open into the narrow, distally closed and  
484 tapering central canal. This implies that (1) this internal canal cannot be homologous to the  
485 axial canal of a stem (in pelmatozoans, the mouth never opens into the stem canal); and (2)  
486 the absence of an internal body cavity and of any anal opening both suggest that, from a  
487 functional point of view, this interpretation is not valid. The suggestion that soft parts were  
488 lying in life over the smooth basal surface of the cone, that is, outside of the theca (see e.g.,  
489 Rozhnov & Kushlina 1994a, b), is incompatible with the body plan of the phylum  
490 Echinodermata. In all echinoderms, the viscera are always housed within the body capsule,  
491 independently of whether it is loosely (e.g., holothurians) or more strongly calcified (most  
492 taxa).

493 In summary, our results do not confirm the identification of *Bolboporites* as the theca of an  
494 eocrinoid. Although most requirements of this interpretation are plausible (e.g., the biserial  
495 pattern of the appendage is similar to that of ambulacral flooring plates; echinoderms with a  
496 single feeding appendage did exist, as well as body capsules consisting of a reduced number  
497 of elements), this hypothesis has to be rejected, because the implied anatomy would be neither  
498 functional (no internal cavity, no viscera, no anus, no hydropore) nor compatible with the  
499 echinoderm body plan (extra-thecal viscera, mouth opening into the stem axial canal).

500

501 *Bolboporites* as an *infrabasal cone*.

502 The overall morphology of *Bolboporites* is strongly reminiscent of similar-looking, cone-  
503 shaped, massive skeletal elements forming the aboral part of the body capsule in some  
504 blastozoans and crinoids. Such aboral (or infrabasal) cones can be made of several tightly  
505 sutured plates, as, for example, in *Cymbionites* and *Peridionites*, both from the Cambrian of  
506 Australia (Whitehouse 1941; Smith 1982). However, single-plated, massive infrabasal cones  
507 have been described in several Cambro-Ordovician eocrinoids (Ubaghs 1963; Clausen 2004;  
508 Allaire *et al.* 2017), as well as in some Late Palaeozoic crinoids (Ettensohn 1975, 1980;  
509 Seilacher & MacClintock 2005; Webster & Kues 2006). As in *Bolboporites*, massive aboral  
510 pelmatozoan cones (plates) also display: (1) a very wide morphological disparity within a



511 same assemblage (see, e.g., Etensohn 1980; Clausen 2004); and (2) a central canal, which is  
512 tapering proximally (i.e., towards the apex of the cone) in stemless taxa (e.g., in the  
513 Pennsylvanian crinoid genus *Paragassizocrinus* Moore & Plummer, 1940; Etensohn 1980).  
514 In contrast, in stemmed taxa, the central canal extends throughout the infrabasal cone and  
515 leads proximally into the axial canal of the stem (see, e.g., Ubaghs 1963; Clausen 2004).

516 However, it seems unlikely that *Bolboporites* corresponds to the infrabasal cone of a  
517 stemless pelmatozoan. The main difficulty is the smooth aspect of its basal surface: in all  
518 pelmatozoans possessing an infrabasal cone, its upper (distal) surface is divided into several  
519 concave areas (facets), separated by ridges and corresponding to the insertion of the plates  
520 (i.e., basals) belonging to the overlying circlet (Ubaghs 1963; Etensohn 1975, 1980; Clausen  
521 2004; Webster & Kues 2006). The absence of such facets in *Bolboporites* implies that its  
522 basal surface was not sutured to any overlying plates and, thus, that this fossil does not  
523 represent an infrabasal cone. This interpretation is further supported by the strongly convex  
524 and particularly high morphology of the basal surface in some specimens of *Bolboporites* (in  
525 particular, in *B. americanus* Billings, 1859; see Clark & Hofmann 1961), which is  
526 incompatible with the presence of a putative overlying basal circlet. Finally, the biserial  
527 appendage articulated to the basal surface of some Russian specimens of *Bolboporites*  
528 (Rozhnov & Kushlina 1994a; Kushlina 2007) clearly demonstrates that this surface was not in  
529 contact with overlying thecal (or calyx) plates.

530

### 531 *Bolboporites* as a spine

532 . Spines are highly differentiated, mobile skeletal elements articulated to the body wall of  
533 echinoderms (see, e.g., Durham *et al.* 1966; Smith 1980b). Although this character gave its  
534 name to the phylum Echinodermata ('spiny skin'), moveable spines indeed occur only in  
535 asterozoans, echinozoans (echinoids), edrioasteroids and stylophorans. In asterozoans,  
536 echinoids and edrioasteroids, the articulation of spines to the body wall is complex, typically  
537 consisting of (1) a concave socket (acetabulum) at the base of the spine; and (2) a  
538 corresponding convex ball (mamelon) located at the summit of a tubercle (Durham *et al.*  
539 1966; Spencer & Wright 1966; Smith 1980b; Holloway & Jell 1983; Guensburg 1988; Lebrun  
540 1998). Attachment and mobility of spines to the body wall are achieved by muscles and/or a  
541 ligamentary catch apparatus (Smith 1980b; Lebrun 1998). Spine movements are controlled by  
542 nerves, forming either a ring around the tubercle (e.g., in echinoids; Durham *et al.* 1966;  
543 Smith 1980b; Lebrun 1998) and/or extending inside the spine itself (e.g., in some ophiuroids;  
544 Lebrun 1998). In cornute stylophorans (e.g., chauvelicystids, *Thoralicystis griffei* (Ubaghs,

545 1970)), spines are articulated to various parts of the body wall (proximal aulacophore,  
546 supracentral area, thecal margin) by rudimentary balls and sockets (Ubaghs 1970, 1983; Lee  
547 *et al.* 2005). In most mitrate stylophorans, the articulation of posterior spines (digital, glossal)  
548 consists of complex balls and sockets (e.g., in anomalocystitids; Ubaghs 1968a; Parsley 1991;  
549 Ruta & Bartels 1998). In some other taxa (e.g., *Balanocystites primus* (Barrande, 1872)), the  
550 posterior spine is connected to the theca by a small column of articulated plates (Lefebvre  
551 1999).

552 Spines are thus distinct from spine-shaped tubercles, which are non-articulated (fixed),  
553 protruding external structures that can be produced by various elements of the body wall (e.g.,  
554 anal plates, calyx or thecal plates, columnals). Tubercles are particularly widespread at  
555 phylum-scale. In blastozoans, spine-shaped expansions of thecal plates have been described in  
556 aristocystitids (e.g., *Calix sedgwicki* Rouault, 1851; *Lepidocalix pulcher* Termier & Termier,  
557 1950; see Chauvel 1941; Makhlof *et al.* 2017), blastoids (e.g., *Thaumatoblastus* Wanner,  
558 1924; *Pteratoblastus* Wanner, 1924; see Beaver *et al.* 1968), eocrinoids (e.g., *Rhopalocystis*  
559 *havliceki* Chauvel, 1978; see Chauvel & Régnault 1986; Allaire *et al.* 2017) and, to a lesser  
560 extent, in glyptocystitids (e.g., *Schizocystis* Jaekel, 1895; Kesling 1968). Strong tubercles also  
561 occur in both cinctans (e.g., *Undatacinctus quadricornuta* (Friedrich, 1993); see Smith &  
562 Zamora 2009) and solutans (e.g., *Girvanicystis batheri* Caster, 1968; see Daley 1992).  
563 Elongate, spine-shaped elements of the body wall also occur in some edrioasteroids  
564 (Guensburg 1988), but they are particularly widespread in Palaeozoic crinoids. In this class,  
565 such a spiny ornamentation has been described on anal plates (e.g., *Stenopeocrinus* Strimple,  
566 1961; *Uperocrinus* Meek & Worthen, 1865; see Ubaghs 1978b; Ausich *et al.* 1999), on  
567 brachials (e.g., *Eirmocrinus* Strimple & Watkins, 1969; *Separocrinus* Knapp, 1969; see  
568 Moore *et al.* 1978; Ausich *et al.* 1999), on tegmental plates (e.g., *Batocrinus* Casseday, 1854;  
569 see Ubaghs 1978b), on calyx plates (e.g., *Calceolispongia* Etheridge, 1915; *Dorycrinus*  
570 Roemer, 1854; see Moore *et al.* 1978; Ubaghs 1978b; Brett 1999), and to a lesser extent, on  
571 stem elements (e.g., *Aethocrinus moorei* Ubaghs, 1969). Elongate spine-shaped tubercles  
572 occur on the proximal brachials of some cornute (e.g., *Reticulocarpos hanusi* Jefferies &  
573 Prokop, 1972; *Nanocarpus milnerorum* Ruta, 1999; Jefferies, 1986; Lefebvre 2003) and most  
574 mitrate stylophorans (e.g., *Chinianocarpos thoralis* Ubaghs, 1961; *Rhenocystis latipedunculata*  
575 Dehm, 1932; Ubaghs 1970; Jefferies 1986; Ruta & Bartels 1998; Lefebvre 2003). Strong  
576 spine-shaped skeletal elements are also present on the aboral surface of some Recent  
577 oreasterid asteroids (e.g., *Pentaceraster mammilatus*, *Protoreaster nodosus* (Linnaeus, 1758);  
578 see Yeltysheva 1955).

579 The cone-shaped morphology of *Bolboporites* is compatible with its interpretation either as  
580 an isolated spine or a tuberculated plate of an echinoderm (Quenstedt 1881; Lindström 1883;  
581 Wanner 1920; Yeltysheva 1955; Régnell 1956; Clark & Hoffman 1961). Both interpretations  
582 imply that (1) the smooth basal surface was facing towards the organism and was either  
583 articulated to it (spine) or part of its body wall (tubercle); and (2) the lateral, strongly  
584 ornamented walls of the cone were external and directed away from the organism. These two  
585 interpretations could explain the wide disparity in size and shape observed in individuals of  
586 *Bolboporites* from a same level (Yeltysheva 1955; Clark & Hoffman 1961). Both  
587 interpretations would be also in good agreement with the non-random distribution of biofilms  
588 produced by encrusting organisms on Russian specimens (Kushlina 2007). When present,  
589 thick putative algal-bacterial biofilms are consistently encrusting the lateral sides of  
590 *Bolboporites*. They never occur on the smooth, convex surface (Kushlina 2007). This pattern  
591 suggests that the biofilms formed when the organism was alive, otherwise biofilms would be  
592 present on all surfaces. The distribution of these encrusting biofilms also suggests that the  
593 lateral sides of the cones were directly in contact with sea water (i.e., lateral sides were  
594 neither buried in the substrate, nor in contact with the body wall). Conversely, the absence of  
595 biofilms on the smooth surface supports the view that the basal part of the cones was not  
596 exposed to the external medium and, thus, probably in contact with or part of the body wall.

597 As pointed out by Yeltysheva (1955), the overall morphology of *Bolboporites* shows  
598 several similarities with the cone-shaped aboral elements of some oreasterid asteroids. For  
599 example, the observation and dissection of Recent specimens of *Pentaceraster mammilatus*  
600 (Fig. 9D,E) showed that a honeycomb pattern is present on the lateral walls of their cone-  
601 shaped abaxial tubercles (Fig. 9A). This sculpture, which is similar to that observed in  
602 *Bolboporites*, was produced by the thick granulose membrane, which forms the aboral part of  
603 the body wall and extends over the cones. However, the dissection of Recent specimens of *P.*  
604 *mammilatus* also showed some major morphological differences between *Bolboporites* and  
605 oreasterid cone-shaped abaxial elements. The most important one is that the basal surface of  
606 oreasterid cones is not smooth and gently convex, but subdivided into several diverging  
607 branches (Fig. 9B), connecting the cone with surrounding plates (Fig. 9C). This situation is  
608 not unique to oreasterid abaxial cones. All echinoderm spine-shaped tubercles are borne by  
609 elements, which are part of the body wall. This implies that tuberculated plates are necessarily  
610 in contact with neighbouring skeletal elements and thus always display facets along their  
611 sutures. As the basal surface of *Bolboporites* is entirely smooth and does not show any

612 evidence of facets, its interpretation as a putative oreasterid-like cone-shaped element has to  
613 be rejected.

614 Finally, although the interpretation of *Bolboporites* as a spine is plausible (cone-shaped  
615 morphology, smooth surface in contact with the body wall, wide morphological disparity,  
616 encrusting organisms restricted to lateral walls), this hypothesis has implications that can be  
617 tested: (1) skeletal evidence supporting an articulation should be present; and (2) soft parts  
618 (muscles, ligaments and/or nerves) were very likely involved, too, and should have left some  
619 traces. Clearly, the basal surface of *Bolboporites* is entirely smooth and does not show any  
620 skeletal evidence suggesting the presence of a socket for articulation onto a putative tubercle  
621 on the body wall. Consequently, if *Bolboporites* was a spine, its articulation was different  
622 from the most widespread mechanism (balls and sockets) occurring in echinoderms (see  
623 above). The only structures occurring on the smooth surface are the two lunules. However,  
624 these two concave areas were apparently the place of insertion for a biserial appendage (see  
625 discussion above; Rozhnov & Kushlina 1994a; Kushlina 2007). Consequently, if *Bolboporites*  
626 was a spine, the small biserial appendage would then have been directed towards the body  
627 wall. In the mitrate stylophoran *Balanocystites primus*, a similar-looking short appendage,  
628 made of a single column of tiny plates connects the single posterior spine (glossal) to the  
629 theca (Lefebvre 1999). By comparison with the situation in *B. primus*, the possibility that  
630 *Bolboporites* was a spine, which was connected to the body wall by a short, biserial,  
631 articulated appendage cannot be ruled out. If this interpretation is correct, it is thus likely that  
632 the smooth aspect of the basal surface of *Bolboporites* is related to the insertion of soft parts  
633 (probably muscles or ligaments) on it. Moreover, by analogy with the situation in some  
634 ophiuroids (see above; Lebrun 1998), it is then possible to interpret the external longitudinal  
635 groove running on the small appendage and extending internally into the central canal of the  
636 cone as the probable course of a nerve.

637 The interpretation of *Bolboporites* as a spine is thus plausible and cannot be refuted on  
638 available evidence. However, its systematic position remains an open question. The frequent  
639 association of *Bolboporites* with skeletal remains of various blastozoans (e.g., cheirocrinids,  
640 *Palaeocystites*) questioned the possibility that it could represent isolated spines of one of them  
641 (Clark & Hoffman 1961). However, none of the blastozoans found in the same localities as  
642 *Bolboporites* in both Baltica and Laurentia shows any evidence suggesting that spines were  
643 articulated to its body wall. Indeed, spines are only known in asterozoans, echinozoans,  
644 edrioasteroids and stylophorans (see above), thus ruling out any putative blastozoan affinities  
645 for *Bolboporites*. The size of *Bolboporites* (from about 2 to 12 mm in height in both North

646 American and Russian specimens; Clark & Hoffman 1961; Rozhnov & Kushlina 1994a)  
647 suggests that putative stylophoran affinities are highly unlikely. In this class, the size of the  
648 theca is generally comprised between 5 and 30 mm, and it rarely exceeds 30 to 40 mm (e.g.,  
649 the largest known mitrate, *Diamphidiocystis drepanon* Kolata & Guensburg, 1979, is about 40  
650 mm wide; Lefebvre 1999). The large size and cone-shaped morphology of *Bolboporites* seem  
651 to be also incompatible with putative edrioasteroid affinities. When preserved, edrioasteroid  
652 spines are consistently consisting of narrow, elongate elements, typically less than 3 mm in  
653 length, which were articulated to ambulacral cover plates and/or skeletal elements of the  
654 pedunculate zone (Holloway & Jell 1983; Guensburg 1988; Guensburg & Sprinkle 1994).

655 Because of their stratigraphic range and palaeobiogeographic distribution in the  
656 Ordovician, asterozoans are more likely candidates: their oldest known representatives have  
657 been documented in Lower Ordovician deposits (Thoral 1935; Blake 2013; Jell 2014; Blake  
658 & Guensburg 2015), and their presence is recorded in Baltica at least from the Dapingian, i.e.,  
659 as early as the oldest known occurrence of *Bolboporites* (Pisera 1994; Hansen *et al.* 2005;  
660 Rozhnov 2005; Blake & Rozhnov 2007; Tinn & Ainsaar 2014). However, *Bolboporites*  
661 clearly does not show any character supporting its interpretation as an isolated asterozoan  
662 spine. The skeletal morphology of Ordovician asterozoans is strongly constrained and, even  
663 when preserved as isolated remains, their plates are highly diagnostic (Pisera 1994; Tinn &  
664 Ainsaar 2014).

665 Echinozoans possibly appeared and diversified in Baltica during the Middle Ordovician,  
666 before spreading to Laurentia in Late Ordovician times (Reich 1999; Smith & Savill 2001;  
667 Lefebvre *et al.* 2013). Baltica has yielded the oldest known occurrences of echinoids  
668 (Darriwilian; Bockelie & Briskeby 1980; Pisera 1994), holothurians (Darriwilian; Reich  
669 2010) and ophiocistioids (Dapingian; Reich 2001; Rozhnov 2005; Reich & Smith 2009). The  
670 stratigraphic range and palaeobiogeographic distribution of echinozoans are thus compatible  
671 with those of *Bolboporites*. However, the presence of typical tubercles in the oldest known  
672 echinoids (including the isolated plates record; Pisera 1994) suggests the existence of  
673 mechanisms for spine articulation comparable to those occurring in younger taxa (i.e., balls  
674 and sockets). Putative echinoid affinities are thus unlikely for *Bolboporites*. Although spines  
675 have not been documented so far in holothurians and ophiocistioids, it cannot be entirely  
676 excluded that *Bolboporites* corresponds to isolated spines of a yet unknown primitive  
677 echinozoan.

678

679 *Bolboporites* as a columnal.

680 The general aspect of *Bolboporites* reminds in some respects the cone-shaped morphology of  
681 some late Cambrian–Early Ordovician pelmatozoan columnals from Utah (Sumrall *et al.*  
682 1997) and Spain (Zamora *et al.* 2009), and thus questions its possible identification as a  
683 highly differentiated stem plate. This interpretation is in good agreement with (1) the  
684 existence of a longitudinal internal canal; (2) the articulation of a biserial appendage on its  
685 basal surface (Rozhnov & Kushlina 1994a; Kushlina 2007); and (3) the morphology of the  
686 lunules. The biconcave depressed area formed by the lunules, as well as the presence of a tiny  
687 orifice opening in between them are morphological features which are reminiscent of  
688 synarthrial articulations in crinoids (Ubaghs 1978a; Donovan 1988; Ausich *et al.* 1999).  
689 Interestingly, synarthrial articulations were present on the distal columnals of some  
690 Ordovician crinoids (e.g., *Ristnacrinus* Öpik, 1934) co-occurring with *Bolboporites* in Baltica  
691 (Donovan 1984).

692 It seems, however, difficult to interpret *Bolboporites* as a highly differentiated, massive  
693 columnal for several reasons. First, in all pelmatozoan echinoderms, columnals display  
694 articulatory facets on their two opposite (proximal and distal) sides, whereas *Bolboporites*  
695 would display only one facet (i.e., on its basal surface). A second difficulty is that columnals  
696 always display a central canal (lumen), which opens on their two opposite sides: such a canal  
697 is present in *Bolboporites*, but it is not in central position and, more importantly, it opens only  
698 on one side. Finally, the strongly convex morphology of the basal surface in many North  
699 American specimens of *Bolboporites* (see Clark & Hofmann 1961) makes their interpretation  
700 as columnals highly improbable.

701

702 *Bolboporites as a holdfast.*

703 Holdfasts are anchoring structures occurring at the distalmost extremity of the stem in  
704 various blastozoans and crinoids (Ubaghs 1972, 1978a; Brett 1981; Ausich *et al.* 1999;  
705 Seilacher & MacClintock 2005). The massive, cone-shaped morphology of *Bolboporites*  
706 shows many similarities with similarly-shaped, isolated pelmatozoan elements (e.g.,  
707 *Oryctoconus*), generally interpreted as holdfasts (Colchen & Ubaghs 1969; Alvaro & Colchen  
708 2002; Seilacher & MacClintock 2005; Zamora *et al.* 2009). The identification of *Bolboporites*  
709 as a putative discoidal holdfast was discussed, but rejected by Rozhnov & Kushlina (1994a).  
710 Their main argument was that, if this fossil was a holdfast, its basal surface would then be  
711 attached (fixed) to the substrate: this orientation is incompatible with the presence of an  
712 appendage articulated to the basal surface of *Bolboporites*. However, it should be stressed that  
713 this base-down orientation occurs only in the case of pelmatozoan discoidal holdfasts tightly

714 and permanently encrusted on firmgrounds and hardgrounds (Ubaghs 1978a; Brett 1981;  
715 Brett *et al.* 1983; Sumrall *et al.* 1997; Rozhnov 2002). The opposite (base-up) orientation of  
716 the cone is observed in most pelmatozoans living on soft substrates and using their distal  
717 holdfasts as an anchor or a grapnel, as, for example, the Ordovician eocrinoid *Balantiocystis*  
718 Chauvel, 1966, and the Devonian crinoid *Ancyrocrinus* Hall, 1862 ('kite strategy'; Ubaghs  
719 1972; Brett 1981; Le Menn 1985; Ausich *et al.* 1999; Alvaro & Colchen 2002; Seilacher &  
720 MacClintock 2005; Zamora *et al.* 2009).

721 All above-listed arguments agreeing with the interpretation of *Bolboporites* as a columnal  
722 remain valid if this fossil is interpreted as a discoidal terminal holdfast (i.e., internal canal;  
723 biserial appendage inserted into the basal surface; lunules forming a facet with a synarthrial-  
724 like articulation). However, if *Bolboporites* is a holdfast, the various issues raised for its  
725 interpretation as a columnal are no longer problematic: it then makes sense that (1) a single  
726 facet is present (on the basal surface); (2) the internal canal does not open distally into the  
727 apex of the holdfast; and (3) the inflated morphology of the basal surface in some specimens  
728 of *B. americanus* is not incompatible with their interpretation as distal holdfasts. Moreover,  
729 the wide morphological disparity observed between specimens of *Bolboporites* from a same  
730 level (Clark & Hofmann 1961; Kushlina 1995) is also in good agreement with its  
731 interpretation as a holdfast: similar large variabilities in shape have been reported in  
732 assemblages of, for example, *Oryctoconus* and grapnel-like holdfasts of *Ancyrocrinus* (Le  
733 Menn 1985; Alvaro & Colchen 2002; Zamora *et al.* 2009). Finally, this interpretation is also  
734 compatible with the occurrence of *Bolboporites* in deposits corresponding to shallow, storm-  
735 generated deposits (see above; Clark & Hofmann 1961; Bockelie 1981; Dronov 2005). In  
736 such environmental conditions, stemmed echinoderms and their anchoring structures are  
737 generally preserved separately (Brett 1981). Organisms were detached from their anchoring  
738 structures probably by autotomy rather than breakages and transported away by storm  
739 currents, whereas their holdfasts were preserved in situ (Donovan 2012). Apart from some  
740 rare exceptions, such as the eocrinoid *Balantiocystis* or the crinoid *Ancyrocrinus* (Ubaghs  
741 1972; Le Menn 1985; Ausich *et al.* 1999), the distalmost part of the stem is unknown in most  
742 pelmatozoans and, conversely, most holdfasts cannot be assigned to any specific taxa (e.g.,  
743 *Aspidocrinus scutelliformis* Hall, 1859, *Oryctoconus*; Ubaghs 1978a; Brett *et al.* 1983;  
744 Sumrall *et al.* 1997; Alvaro & Colchen 2002; Seilacher & MacClintock 2005; Zamora *et al.*  
745 2009).

746 The interpretation of *Bolboporites* as a discoidal holdfast has also several implications, that  
747 can be tested: (1) the biserial appendage inserting on the lunules would thus probably

748 correspond to the distal-most columnals of a pelmatozoan stem; and (2) if *Bolboporites* was  
749 used as an anchor, it was thus at least partly buried into the sediment. If *Bolboporites* was a  
750 distal holdfast, the presence of two lunules in all specimens suggests that a dimeric stem was  
751 articulated to it. This interpretation is further supported by the observation of a biserial  
752 appendage in at least some better preserved individuals from Russia (Rozhnov & Kushlina  
753 1994a; Kushlina 2007). Although most Ordovician pelmatozoans possessed holomeric stems  
754 (i.e., formed by a single column of plates), tetra-, penta- and hexameric appendages have been  
755 also described in several crinoids (e.g., *Aethocrinus moorei*, *Ramseyocrinus* Bates, 1968;  
756 Ubaghs 1969, 1983; Donovan 1984, 1985), as well as in some echinosphaeritid and  
757 hemicosmitid blastozoans (Jaekel 1899; Bockelie 1981, 1982; Parsley 1998). Dimeric distal  
758 stems are the rule in Ordovician solutans (Caster 1968; Ubaghs 1970; Lefebvre *et al.* 2012;  
759 Noailles *et al.* 2014). Although they possibly retained an attached post-metamorphic stage,  
760 Ordovician solutans were vagile and their stem did not possess any distal discoidal holdfast.  
761 With the exception of solutan elements, only few occurrences of tri- and dimeric columnals  
762 were documented in Ordovician deposits, and all of them have been assigned to crinoids  
763 possibly related to *Ectenocrinus* Miller, 1889 (e.g., Donovan 1985). Consequently, the  
764 existence of Ordovician pelmatozoans with a stem comprising dimeric columnals supports the  
765 identification of *Bolboporites* as a possible distal holdfast articulated to a biserial appendage.

766 However, contrary to the situation in all echinoderm stem-like appendages, the biserial  
767 structure articulated to the basal surface of *Bolboporites* does not contain any lumen (internal  
768 central canal), but an external groove (Rozhnov & Kushlina 1994a). This external groove,  
769 which probably housed soft parts, communicates with the longitudinal internal canal of  
770 *Bolboporites*. In all stemmed echinoderms, the lumen contains coeloms associated with the  
771 extraxial part of the body wall (i.e., somatocoels) and, generally, extensions of the nervous  
772 system (Ubaghs 1978a; Heinzeller & Welsh 1994; David *et al.* 2000; Mooi & David 2008).  
773 The topology observed in *Bolboporites* and its associated appendage thus strongly departs  
774 from the situation in pelmatozoan stems (external vs. internal soft parts). This implies that the  
775 biserial structure articulated to *Bolboporites* cannot be interpreted as (part of) a stem-like  
776 appendage and, consequently, that *Bolboporites* was not a distal holdfast. This conclusion is  
777 confirmed by the distribution of biofilms produced by encrusting organisms over the body  
778 wall of *Bolboporites* (see above; Kushlina 2007). If this fossil was a discoidal terminal  
779 holdfast, comparison with similar structures in pelmatozoans (Ausich *et al.* 1999; Seilacher &  
780 MacClintock 2005) suggests that in life, a large part of the cone would have been at least  
781 partly buried into and/or in permanent contact with the substrate. This life orientation is not



782 compatible with the observed distribution of epibionts, which produced extensive films on the  
783 lateral walls of *Bolboporites*, but are absent from its basal surface (Kushlina 2007).

784 Consequently, although the interpretation of *Bolboporites* as a discoidal distal holdfast is  
785 plausible (e.g., massive cone-shaped morphology, wide morphological disparity, articulation  
786 to a dimeric appendage; see above), this identification has to be rejected because the structure  
787 articulated to its basal surface is not a stem-like appendage (no lumen, external groove  
788 housing soft parts). Further, the implied life orientation is not confirmed by the distribution of  
789 epibionts on the cones.

790

791

## 792 **Conclusions**

793

794 Our results not only confirmed the presence of stereomic microstructure in *Bolboporites* (and  
795 thus its echinoderm affinities), but they also showed that this fossil is a single, previously  
796 microporous, calcitic skeletal element, without any internal macrostructure, except a narrow  
797 longitudinal canal opening through a tiny orifice on the basal surface. These results combined  
798 with all previous descriptions of *Bolboporites* have made it possible to critically discuss  
799 several hypotheses about its nature (e.g., theca, basal cone, spine, columnal, holdfast) and its  
800 putative affinities within echinoderms (e.g., asterozoans, blastozoans, crinoids, echinozoans,  
801 stylophorans). Most interpretations could be rejected, because they comply with only part of  
802 available evidences. Although the identification of *Bolboporites* as a spine remains  
803 questionable, it represents the most parsimonious - and likely - interpretation. The precise  
804 affinities of *Bolboporites* remain difficult to assess and it is tentatively assigned here to an  
805 unknown, possibly basal echinozoan. As this was the case for other problematic fossils (e.g.,  
806 conodonts, machaeridians), future discoveries of fully articulated specimens showing  
807 *Bolboporites* elements in connection with their host organism will probably help in revealing  
808 their actual nature and affinities within echinoderms.

809

810

## 811 **Acknowledgments**

812

813 This paper is a contribution to the International Geoscience Programme (IGCP) Project 653 –  
814 The onset of the Great Ordovician Biodiversification Event, and of the team 'Biosignatures,  
815 Vie Primitive' of UMR CNRS 5276 LGLTPE. The paper is also a contribution to the revision

816 of volumes S and U of the *Treatise on Invertebrate Paleontology*. The authors are particularly  
817 grateful to Sergei V. Rozhnov (Palaeontological Institute of the Russian Academy of  
818 Sciences, Moscow) for providing numerous, well-preserved specimens of *Bolboporites* sp. for  
819 this study, and for insightful and constructive discussions on their systematic affinities. Hans-  
820 Arne Nakrem and Franz-Josef Lindemann (Natural History Museum, Oslo) are thanked for  
821 access to the Norwegian material of *Bolboporites* and *Coelosphaeridium*, and Michel Creuzé  
822 des Châtelliers and Blandine Bärtschi (Lyon 1 University, Villeurbanne) for access and  
823 dissection of specimens of the Recent spiny starfish *Pentaceraster mammilatus*. Jih-Pai Lin  
824 (National Taiwan University) is also acknowledged for having made available specimens of  
825 *Timorocidaris* for comparison. Frédéric Herbst (UMR6303 ICB, Burgundy University, Dijon)  
826 acquired the EBSD data. This study also benefited from useful comments from and/or  
827 discussions with Daniel B. Blake (University of Illinois, Champaign), Gilles Cuny and  
828 Vincent Perrier (Lyon 1 University, Villeurbanne), Georgy Mirantsev (Palaeontological  
829 Institute of the Russian Academy of Sciences, Moscow), Elise Nardin (Observatoire Midi-  
830 Pyrénées, Toulouse), Colin D. Sumrall (University of Tennessee, Knoxville), and Gary D.  
831 Webster (Washington State University, Pullman). Finally, Thomas E. Guensburg (Field  
832 Museum, Chicago) and Stephen K. Donovan (Naturalis, Leiden) are greatly thanked for their  
833 constructive and helpful reviews.

834

835

## 836 **References**

837

- 838 Allaire, N., Lefebvre, B., Nardin, E., Martin, E.L.O., Vaucher, R. & Escarguel, G. (2017) Morphological  
839 disparity analysis and systematic revision of the eocrinoid genus *Rhopalocystis* (Echinodermata,  
840 Blastozoa) from the Lower Ordovician of the central Anti-Atlas (Morocco). *Journal of Paleontology*,  
841 91, 685–714.
- 842 Alvaro, J.J. & Colchen, M. (2002) Earliest Ordovician pelmatozoan holdfasts from western Europe: the  
843 *Oryctoconus* problem revisited. *Eclogae Geologicae Helvetiae*, 95, 451–459.
- 844 Ami, H.M. (1896) Preliminary lists of the organic remains occurring in the various geological formations  
845 comprised in the southwest quartersheet map of the eastern townships of the Province of Quebec.  
846 *Geological Survey of Canada, Annual Report*, 7, 113–157.
- 847 Audouin, V. (1826) Explication des planches d'échinodermes de l'Égypte et de la Syrie publiées par Jules-  
848 César Savigny, membre de l'Institut. In: *Description de l'Égypte ou Recueil des Observations et des*  
849 *Recherches qui ont été faites pendant l'Expédition de l'Armée Française*. Imprimerie impériale (1809),  
850 Paris, pp. 203-212
- 851 Ausich, W.I., Brett, C.E., Hess, H. & Simms, M.J. (1999) Crinoid form and function. In: Hess, H., Ausich,  
852 W.I., Brett, C.E. & Simms, M.J. (Eds.), *Fossil Crinoids*. Cambridge University Press, Cambridge, pp.  
853 3–30.

- 854 Baarli, B.G. (2008) *Fossilboka*. Forlaget Vett & Viten AS, Nesbru, 367 pp.
- 855 Barrande, J. (1872) *Système Silurien du Centre de la Bohême. Supplément au Volume I. Trilobites,*  
856 *Crustacés divers et Poissons*. Bellman, Prague, 647 pp.
- 857 Bassler, R.S. (1911) The Early Paleozoic Bryozoa of the Baltic provinces. *United States National Museum*  
858 *Bulletin*, 77, 1–49.
- 859 Bassler, R.S. (1915) Bibliographic index of American Ordovician and Silurian fossils. Volume 1. *United*  
860 *States National Museum Bulletin*, 92, 1–718.
- 861 Bates, D.E.B. (1968) On ‘*Dendrocrinus*’ *cambriensis* Hicks, the earliest known crinoid. *Palaeontology*, 11,  
862 406–409.
- 863 Bather, F.A. (1920) Echinoid or crinoid? *Geological Magazine*, 57, 371–372.
- 864 Beaver, H.H., Fay, R.O., Macurda, D.B., Moore, R.C. & Wanner, J. (1968) Blastoids. In: Moore, R.C.  
865 (Ed.), *Treatise on Invertebrate Paleontology, Echinodermata 1(2)*. Geological Society of America,  
866 Boulder & University of Kansas Press, Lawrence, pp. S297–S455.
- 867 Berg-Madsen, V. (1986) Middle Cambrian cystoid (*sensu lato*) columnals from Bornholm, Denmark.  
868 *Lethaia*, 19, 67–80.
- 869 Billings, E. (1859) The fossils of the Chazy Limestone with descriptions of new species. *The Canadian*  
870 *Naturalist and Geologist*, 4, 426–470.
- 871 Bischoff, W.D., Mackenzie, F.T., Bishop, F.C. (1993) Diagenetic stabilization pathways of magnesian  
872 calcites. *Carbonates & Evaporites*, 8, 82–89.
- 873 Blake, D.B. (2013) Early asterozoan (Echinodermata) diversification: a paleontologic quandary. *Journal of*  
874 *Paleontology*, 87, 353–372.
- 875 Blake, D.B. & Guensburg, T.E. (2015) The class Somasteroidea (Echinodermata, Asterozoa): morphology  
876 and occurrence. *Journal of Paleontology*, 89, 465–486.
- 877 Blake, D.B. & Rozhnov, S.V. (2007) Aspects of life mode among Ordovician asteroids: implications of  
878 new specimens from Baltica. *Acta Palaeontologica Polonica*, 52, 519–533.
- 879 Bockelie, J.F. (1981) The Middle Ordovician of the Oslo region, Norway, 30. The eocrinoid genera  
880 *Cryptocrinites*, *Rhipidocystis* and *Bockia*. *Norsk Geologisk Tidsskrift*, 61, 123–147.
- 881 Bockelie, J.F. (1982) Morphology, growth and taxonomy of the Ordovician rhombiferan *Caryocystites*.  
882 *Geologiska Föreningens I Stockholm Förhandlingar*, 103, 491–498.
- 883 Bockelie, J.F. & Briskeby, P.I. (1980) The presence of a bothriocidarid (Echinoid) in the Ordovician of  
884 Norway. *Norsk Geologisk Tidsskrift*, 60, 89–91.
- 885 Brainerd, E. (1891) The Chazy Formation in the Champlain Valley. *Bulletin of the Geological Society of*  
886 *America*, 2, 293–300.
- 887 Brainerd, E. & Seely, H.M. (1888) The original Chazy rocks. *American Geologist*, 2, 323–330.
- 888 Brainerd, E. & Seely, H.M. (1896) The Chazy of Lake Champlain. *American Museum of Natural History*  
889 *Bulletin*, 8, 305–315.
- 890 Brett, C.E. (1981) Terminology and functional morphology of attachment structures in pelmatozoan  
891 echinoderms. *Lethaia*, 14, 343–370.
- 892 Brett, C.E. (1999) Middle Devonian Windom Shale of Vincent, New York, USA. In: Hess, H., Ausich,  
893 W.I., Brett, C.E. & Simms, M.J. (Eds.), *Fossil Crinoids*. Cambridge University Press, Cambridge, pp.  
894 122–128.
- 895 Brett, C.E., Liddell, W.D. & Derstler, K.L. (1983) Late Cambrian hard substrate communities from  
896 Montana/Wyoming: the oldest known hardground encrusters. *Lethaia*, 16, 281–289.
- 897 Brett, C.E., Moffat, H.A. & Taylor, W.L. (1997) Echinoderm taphonomy, taphofacies, and Lagerstätten.  
898 *Paleontological Society Papers*, 3, 147–190.
- 899 Briggs, D.E.G., Siveter, D.J., Siveter, D.J., Sutton, M.F. & Rahman, I.A. (2017) An edrioateroid from the  
900 Silurian Herefordshire Lagerstätte of England reveals the nature of the water vascular system in an  
901 extinct echinoderm. *Proceedings of the Royal Society B*, 284, 20171189.
- 902 Bronn, H.G. (1849) *Index Palaeontologicus oder Übersicht der bis jetzt bekannten fossilen Organismen*. E.  
903 Schweizerbart'sche Verlagshandlung und Druckerei, Stuttgart, 1381 pp.

- 904 Bronn, H.G. (1851–1856) Systematische Übersicht der fossilen Pflanzen und Thiere nach ihrer  
905 geologischen Verbreitung. Schlüssel-Tabellen oder Claves einzelner Klassen. Alphabetisches Register.  
906 In: Bronn, H.G. & Roemer, F. (Eds.), *Lethaea Geognostica oder Abbildung und Beschreibung der für*  
907 *die Gebirgs-Formationen Bezeichnendsten Versteinerungen*, Volume 1.  
908 Schweizerbart'sche Verlagsbuchhandlung und Druckerei, Stuttgart, pp. 1–204.
- 909 Butts, C. (1940) Geology of the Appalachian Valley in Virginia, part 1. Geologic text and illustrations.  
910 *Virginia Geological Survey Bulletin*, 52, 1–568.
- 911 Casseday, S.A. (1854) Beschreibung eines neuen Crinoideengeschlechts Nordamerika. *Zeitschrift der*  
912 *Deutschen Geologischen Gesellschaft*, 6, 237–242.
- 913 Caster, K.E. (1968) Homoiostelea. In: Moore, R.C (Ed.), *Treatise on Invertebrate Paleontology,*  
914 *Echinodermata 1(2)*. Geological Society of America, Boulder & University of Kansas Press, Lawrence,  
915 pp. S581–S627.
- 916 Chauvel, J. (1941) Recherches sur les cystoïdes et les carpoïdes armoricains. *Mémoires de la Société*  
917 *géologique et minéralogique de Bretagne*, 5, 1–286.
- 918 Chauvel, J. (1966) *Echinodermes de l'Ordovicien du Maroc*. Editions du CNRS, Paris, 120 pp.
- 919 Chauvel, J. (1978) Compléments sur les échinodermes du Paléozoïque marocain (diploporites, éocrinoïdes,  
920 édrioastéroïdés). *Notes du Service géologique du Maroc*, 39, 27–78.
- 921 Chauvel, J. & Régnault, (1986) Variabilité du genre *Rhopalocystis* Ubaghs, éocrinoïde du Trémadocien de  
922 l'Anti-Atlas marocain. *Geobios*, 19, 863–870.
- 923 Checa, A.G., Esteban-Delgado, F.J., Ramirez-Rico, J., Rodriguez-Navarro, A.B. (2009) Crystallographic  
924 reorganization of the calcitic prismatic layer of oysters. *Journal of Structural Biology*, 167, 261–270.
- 925 Clark, A.M. & Rowe, F.W.E. (1971) *Monograph of Shallow-Water Indo-West Pacific Echinoderms*. The  
926 Natural History Museum, London, 238 pp.
- 927 Clark, T.H. (1944) Unfolded Palaeozoic rocks of the St. Lawrence Lowlands. In: Dresser, J.A. & Denis,  
928 T.C. (Eds.), *The Geology of Quebec, Volume 2. Descriptive Geology*. Quebec Department of Mines,  
929 Geological Report, 20, pp. 250–291.
- 930 Clark, T.H. (1952) Montreal area, Laval and Lachine map areas. *Quebec Department of Mines, Geological*  
931 *Report*, 46, 1–159.
- 932 Clark, T.H. & Hofmann, H.J. (1961) *Bolboporites americanus* in the Chazy of Southern Quebec.  
933 *Transactions of the Royal Society of Canada*, 55, 13–28.
- 934 Clausen, S. (2004) New Early Cambrian eocrinoids from the Iberian Chains (NE Spain) and their role in  
935 nonreefal benthic communities. *Eclogae Geologicae Helveticae*, 97, 371–379.
- 936 Colchen, M. & Ubaghs, G. (1969) Sur des restes d'échinodermes(?) du Cambro-Ordovicien de la Sierra de  
937 la Demanda (Burgos-Logrono, Espagne). *Bulletin de la Société géologique de France*, 11, 649–654.
- 938 Cusack, M (2016) Biomineral electron backscatter diffraction for palaeontology. *Palaeontology*, 59, 171–  
939 179.
- 940 Daley, P.E.J. (1992) The anatomy of the solute *Girvanicystis batheri* (?Chordata) from the Upper  
941 Ordovician of Scotland and a new species of *Girvanicystis* from the Upper Ordovician of south Wales.  
942 *Zoological Journal of the Linnean Society*, 105, 353–375.
- 943 David, B. & Mooi, R. (1996) Embryology supports a new theory of skeletal homologies for the phylum  
944 Echinodermata. *Comptes-Rendus de l'Académie des Sciences, Paris, Sciences de la vie/Life sciences*,  
945 319, 577–584.
- 946 David, B. & Mooi, R. (1999) Comprendre les échinodermes: la contribution du modèle extraxial-axial.  
947 *Bulletin de la Société géologique de France*, 170, 91–101.
- 948 David, B., Lefebvre, B., Mooi, R. & Parsley, R. (2000) Are homalozoans echinoderms? An answer from  
949 the extraxial-axial theory. *Paleobiology*, 26, 529–555.
- 950 Dehm, R. (1932) Cystoideen aus dem rheinischen Unterdevon. *Neues Jahrbuch für Mineralogie, Geologie*  
951 *und Paläontologie, Beilage-Band, Abteilung A*, 69, 63–93.
- 952 Dominguez, P., Jacobson, A.G. & Jefferies, R.P.S. (2002) Paired gill slits in a fossil with a calcite skeleton.  
953 *Nature*, 417, 841–844.

- 954 Donovan, S.K. (1984) *Ramseyocrinus* and *Ristnacrinus* from the Ordovician of Britain. *Palaeontology*, 27,  
955 623–634.
- 956 Donovan, S.K. (1985) Biostratigraphy and evolution of crinoid columnals from the Ordovician of Britain.  
957 In: Keegan, B.F. & O'Connor, B.D.S. (Eds.), *Echinodermata: Proceedings of the Fifth International*  
958 *Echinoderm Conference, Galway, 24-29 September, 1984*. Balkema, Rotterdam, pp. 19–24.
- 959 Donovan, S.K. (1988) Functional morphology of synarthrial articulations in the crinoid stem. *Lethaia*, 21,  
960 169–175.
- 961 Donovan, S.K. (1991) The taphonomy of echinoderms: calcareous multi-element skeletons in the marine  
962 environment. In: Donovan, S.K. (Ed.), *The Processes of Fossilization*. Belhaven Press, London, pp.  
963 241–269.
- 964 Donovan, S.K. (2012) Was autotomy a pervasive adaptation of the crinoid stalk during the Paleozoic?  
965 *Geology*, 40, 867–870.
- 966 Donovan, S.K. (2018) The internal morphology of primary spines of extant regular echinoids in the tropical  
967 western Atlantic: a SEM atlas. *Swiss Journal of Palaeontology*, 137, 363–377.
- 968 Dronov, A. (2005) Introduction to the geology of the St. Petersburg region. In: Dronov, A., Tolmacheva,  
969 T., Raevskaya, E. & Nestell, M. (Eds.), *Cambrian and Ordovician of St. Petersburg area. Guidebook of*  
970 *the pre-conference field trip*. St. Petersburg State University, Saint-Petersburg, pp. 2–15.
- 971 Durham, J.W., Fell, H.B., Fischer, A.G., Kier, P.M., Melville, R.V., Pawson, D.L. & Wagner, C.D. (1966)  
972 Echinoids. In: Moore, R.C. (Ed.), *Treatise on Invertebrate Paleontology, Echinodermata 3(1–2)*.  
973 Geological Society of America, Boulder & University of Kansas Press, Lawrence, pp. U211–U640.
- 974 Eichwald, E. von (1857) *Beitrag zur geographischen Verbreitung der fossilen Thiere Russlands. Alte*  
975 *Period*. Buchdruckerei der Kaiserlichen Universität, Moscow, 242 pp.
- 976 Eichwald, E. von (1860) *Lethaea Rossica ou Paléontologie de la Russie. Premier Volume. Première*  
977 *Section de l'Ancienne Période*. Schweitzerbart, Stuttgart, 1657 pp.
- 978 Etheridge, R. (1915) Western Australian Carboniferous fossils, chiefly from Mount Marmion, Lennard  
979 River, West Kimberley. *Bulletin - Geological Survey of Western Australia*, 58, 7–49.
- 980 Etnensohn, F.R. (1975) The autecology of *Agassizocrinus lobatus*. *Journal of Paleontology*, 49, 1044–1061.
- 981 Etnensohn, F.R. (1980) *Paragassizocrinus*: systematics, phylogeny and ecology. *Journal of Paleontology*,  
982 54, 978–1007.
- 983 Federov, P. (2003) Lower Ordovician mud mounds from the St. Petersburg region, northwestern Russia.  
984 *Bulletin of the Geological Society of Denmark*, 50, 125–137.
- 985 Fischer von Waldheim, G. (1829) Prodrömus Petromatognosiae Animalium Systematicae Continens,  
986 Bibliographiam Animalium Fossilium. *Nouveaux Mémoires de la Société Impériale des Naturalistes de*  
987 *Moscou*, 1, 301–374.
- 988 Friedrich, W.P. (1993) Systematik und Funktionsmorphologie mittelkambrischer Cincta (Carpoidea,  
989 Echinodermata). *Beringeria*, 7, 1–190.
- 990 Fromentel, E. de (1861) Introduction à l'étude des Polypiers fossiles. *Mémoires de la Société d'Emulation*  
991 *du Département du Doubs*, 5, 1–357.
- 992 Génot, P. & Granier, B. (2011) Cenozoic Dasycladales. A photo-atlas of Thanetian, Ypresian and  
993 Bartonian species from the Paris Basin. *Carnets de Géologie, Special Paper*, 2011/1, 1–44.
- 994 Gislén, T. (1947) On the Haplozoa and the interpretation of *Peridionites*. *Zoologiska Bidrag från Uppsala*,  
995 25, 402–408.
- 996 Gorzelak, P. & Zamora, S. (2013) Stereom microstructures of Cambrian echinoderms revealed by  
997 cathodoluminescence (CL). *Palaeontologia Electronica*, 16.3.32A, 1–17.
- 998 Gorzelak, P., Krzykowski, T., Stolarski, J. (2016) Diagenesis of echinoderm skeletons: constraints on  
999 paleoseawater Mg/Ca reconstructions. *Global and Planetary Change*, 144, 142–157.
- 1000 Guensburg, T.E. (1988) Systematics, functional morphology, and life modes of Late Ordovician  
1001 edrioasteroids, Orchard Creek Shale, southern Illinois. *Journal of Paleontology*, 62, 110–126.

- 1002 Guensburg, T.E. & Sprinkle, J. (1994) Revised phylogeny and functional interpretation of the  
1003 Edrioasteroidea based on new taxa from the Early and Middle Ordovician of western Utah. *Fieldiana,*  
1004 *Geology*, 29, 1–43.
- 1005 Hall, J. (1847) *Paleontology of New York. Volume 1. Containing Descriptions of the Organic Remains of*  
1006 *the Lower Division of the New York System (equivalent to the Lower Silurian Rocks of Europe)*. Van  
1007 Benthuyssen, New York, 338 pp.
- 1008 Hall, J. (1859) Descriptions and figures of the organic remains of the lower Helderberg group and the  
1009 Oriskany sandstone. *New York Geological Survey*, 3, 1–532.
- 1010 Hall, J. (1862) Preliminary notice of some species of Crinoidea from the Waverly sandstone series of  
1011 Summit Co., Ohio, supposed to be of the age of the Chemung group of New York. *Annual report on the*  
1012 *New York State Museum of Natural History*, 17, 50–60.
- 1013 Hansen, T., Bruton, D.L. & Jakobsen, S.L. (2005) Starfish from the Ordovician of the Oslo region,  
1014 Norway. *Norwegian Journal of Geology*, 85, 209–216.
- 1015 Heinzeller, T. & Welsch, U. (1994) Crinoidea. In: Harrison, F.W. & Ruppert, E.W. (Eds.), *Microscopic*  
1016 *Anatomy of Invertebrates*. Wiley, New York, pp. 9–148.
- 1017 Herbert, B. & Ettensohn, F.R. (2018) What is *Edriocrinus*? *Geological Society of America Abstracts with*  
1018 *Programs*, 50, 36–9.
- 1019 Hess, H. (1999) Permian. In: Hess, H., Ausich, W.I., Brett, C.E. & Simms, M.J. (Eds.), *Fossil Crinoids*.  
1020 Cambridge University Press, Cambridge, pp. 160–163.
- 1021 Holloway, D.J. & Jell, P.A. (1983) Silurian and Devonian edrioasteroids from Australia. *Journal of*  
1022 *Paleontology*, 57, 1001–1016.
- 1023 Jaekel, O. (1895) Über die Organisation der Cystoideen. *Deutsche Zoologische Gesellschaft*  
1024 *Verhandlungen*, 5, 109–121.
- 1025 Jaekel, O. (1899) *Stammgeschichte der Pelmatozoen. Erster Band: Thecoidea und Cystoidea*. Springer,  
1026 Berlin, 442 pp.
- 1027 Jefferies, R.P.S. (1986) *The Ancestry of the Vertebrates*. British Museum (Natural History), London, 376  
1028 pp.
- 1029 Jefferies, R.P.S. & Prokop, R.J. (1972) A new calcichordate from the Ordovician of Bohemia and its  
1030 anatomy, adaptations and relationships. *Biological Journal of the Linnean Society*, 4, 69–115.
- 1031 Jell, P.A. (2014) A Tremadocian asterozoan from Tasmania and a late Llandovery edrioasteroid from  
1032 Victoria. *Alcheringa*, 38, 528–540.
- 1033 Jones, G. C. & Jackson, B. (1993) *Infrared Transmission Spectra of Carbonate Minerals*. Chapman & Hall,  
1034 London, 254 pp.
- 1035 Kato, M., Goel, R.K. & Srivastava, S.S. (1987) Ordovician Algae from Spiti, India. *Journal of the Faculty*  
1036 *of Sciences, Hokkaido University*, 22, 313–323.
- 1037 Kesling, R.V. (1968) Cystoids. In: Moore, R.C (Ed.), *Treatise on Invertebrate Paleontology,*  
1038 *Echinodermata 1(1)*. Geological Society of America, Boulder & University of Kansas Press, Lawrence,  
1039 pp. S85–S267.
- 1040 Kjerulf, T. (1865) *Veiviser Ved Geologiske Excursioner i Christiania Omegn*. Brøgger & Christie's  
1041 Bogtrykkeri, Christiania, 43 pp.
- 1042 Knapp, W.D. (1969) Declinida, a new order of late Paleozoic inadunate crinoids. *Journal of Paleontology*,  
1043 43, 340–391.
- 1044 Kolata, D.R. & Guensburg, T.E. (1979) *Diamphidiocystis*, a new mitrate “carpoid” from the Cincinnati  
1045 (Upper Ordovician) Maquoketa Group in southern Illinois. *Journal of Paleontology*, 53, 1121–1135.
- 1046 Kolata, D.R., Frest, T.J. & Mapes, R.H. (1991) The youngest carpoid: occurrence, affinities and life mode  
1047 of a Pennsylvanian (Morrowan) mitrate from Oklahoma. *Journal of Paleontology*, 65, 844–855.
- 1048 Kouchinsky, A., Bengtson, S., Runnegar, B., Skovsted, C., Steiner, M. & Vedrasco, M. (2012) Chronology  
1049 of early Cambrian biomineralization. *Geological Magazine*, 149, 221–251.
- 1050 Kushlina, V.B. (1995) The systematic position and composition of the genus *Bolboporites* (Echinodermata,  
1051 Eocrinoidea). *Paleontological Journal*, 29, 46–61.

- 1052 Kushlina, V.B. (2006) Biting traces on echinoderms from the Ordovician of the St. Petersburg region  
1053 (Russia). In: Mikuláš, R. & Rindsberg, A.K. (Eds.), *Abstract Book: Workshop on Ichnotaxonomy – III,*  
1054 *Prague and Moravia, Czech Republic.* Institute of Geology & Academy of Sciences of the Czech  
1055 Republic, Prague, pp. 12–14.
- 1056 Kushlina, V.B. (2007) Possible algal-bacterial biofilms on eocrinoids from the Ordovician of the St.  
1057 Petersburg region (Russia). *Acta Palaeontologica Sinica*, 46 (Suppl.), 237–240.
- 1058 Lamarck, J.B. M. de (1816) *Histoire Naturelle des Animaux sans Vertèbres. Tome Second.* Verdière, Paris,  
1059 568 pp.
- 1060 Lebrun, P. (1998) Oursins. *Minéraux & Fossiles, hors-série* 8, 1–112.
- 1061 Lee, S.B., Lefebvre, B. & Choi, D.K. (2005) Latest Cambrian cornutes (Echinodermata, Stylophora) from  
1062 the Taebaeksan Basin, Korea. *Journal of Paleontology*, 79, 139–151.
- 1063 Lefebvre, B. (1999) *Stylophores (Cornuta, Mitrata) : Situation au sein du Phylum des Echinodermes et*  
1064 *Phylogénèse*, Unpublished PhD thesis, Lyon 1 University, 630 pp.
- 1065 Lefebvre, B. (2003) Functional morphology of stylophoran echinoderms. *Palaeontology*, 46, 511–555.
- 1066 Lefebvre, B. (2014) Reinterpretation of the problematic Ordovician genus *Bolboporites* (?Echinodermata)  
1067 as a calcareous alga. *Programme and Abstracts, 58th Annual Meeting of the Palaeontological*  
1068 *Association, Leeds*, 79.
- 1069 Lefebvre, B. (2017) Réinterprétation de *Bolboporites*, un fossile ordovicien énigmatique. *Journal de*  
1070 *l'Association Paléontologique Française*, 72, 30.
- 1071 Lefebvre, B. & Lerosey-Aubril, R. (2018) Laurentian origin of solutan echinoderms: new evidence from  
1072 the Guzhangian (Cambrian Series 3) Weeks Formation of Utah, USA. *Geological Magazine*, 155,  
1073 1190–1204.
- 1074 Lefebvre, B., Derstler, K. & Sumrall, C.D. (2012) A reinterpretation of the solutan *Plasiacystis mobilis*  
1075 (Echinodermata) from the Middle Ordovician of Bohemia. In: Kroh, A. & Reich, M. (Eds.),  
1076 *Echinoderm Research 2010. Proceedings of the Seventh European Conference on Echinoderms,*  
1077 *Göttingen, Germany, 2-9 October 2010. Zoosymposia*, 7, 287–306.
- 1078 Lefebvre, B., Sumrall, C.D., Shroat-Lewis, R.A., Reich, M., Webster, G.D., Hunter, A.W., Nardin, E.,  
1079 Rozhnov, S.V., Guensburg, T.E., Touzeau, A., Noailles, F. & Sprinkle, J. (2013) Palaeobiogeography of  
1080 Ordovician echinoderms. In: Harper, D.A.T & Servais, T. (Eds.), *Early Palaeozoic Biogeography and*  
1081 *Palaeogeography. Geological Society, London, Memoirs*, 38, 173–198.
- 1082 Le Menn, J. (1985) Les crinoïdes du Dévonien inférieur et moyen du Massif armoricain. Systématique,  
1083 paléobiologie, évolution, biostratigraphie. *Mémoires de la Société Géologique et Minéralogique de*  
1084 *Bretagne*, 30, 1–268.
- 1085 Lindström, G. (1883) Index to generic names applied to the corals of the Palaeozoic formations. *Bihang till*  
1086 *Kongliga Svenska vetenskaps-akademiens Handlingar*, 8, 3–14.
- 1087 Linnaeus, C. (1758) *Systema Naturae per Regna Tria Naturae. Secundum Classes, Ordines, Genera,*  
1088 *Species, cum Characteribus, Differentiis, Synonymis, Locis. Tomus I. Pars II.* Editio Duodecima  
1089 Reformata Laurentii Salvii, Holmiae, pp. 533–1327.
- 1090 Logan, W.E., Murray, A., Hunt, T.S. & Billings, E. (1863) *Report of Progress from its commencement to*  
1091 *1863.* Geological Survey of Canada, Montreal, 983 pp.
- 1092 Makhlof, Y., Lefebvre, B., Nardin, E., Nedjari, A. & Paul, C.R.C. (2017) *Lepidocalix pulcher* Termier  
1093 and Termier, 1950 (Echinodermata, Diploporita) from the Middle Ordovician of northern Algeria:  
1094 taxonomic revision and palaeoecological implications. *Acta Palaeontologica Polonica*, 62, 299–310.
- 1095 Meek, F.B. & Worthen, A.H. (1865) Description of new species of Crinoidea, etc., from the Palaeozoic  
1096 rocks of Illinois and some of the adjoining states. *Proceedings of the National Academy of Sciences*, 17,  
1097 143–155.
- 1098 Miller, S.A. (1889) *North American Geology and Palaeontology for the Use of Amateurs, Students, and*  
1099 *Scientists.* Western Methodist Book Concern, Cincinnati, 793 pp.

- 1100 Milne-Edwards, H. & Haime, J. (1851) Monographie des Polypiers fossiles des terrains paléozoïques,  
1101 précédée d'un tableau général de la classification des Polypes. *Archives du Muséum d'Histoire*  
1102 *Naturelle*, 5, 1–502.
- 1103 Mooi, R. & David, B. (1997) Skeletal homologies of echinoderms. *Paleontological Society Papers*, 3, 305–  
1104 335.
- 1105 Mooi, R. & David, B. (1998) Evolution within a bizarre phylum: homologies of the first echinoderms.  
1106 *American Zoologist*, 38, 965–974.
- 1107 Mooi, R. & David, B. (2008) Radial symmetry, the anterior/posterior axis, and echinoderm Hox genes.  
1108 *Annual Review of Ecology, Evolution, and Systematics*, 39, 43–62.
- 1109 Moore, R.C. (1978) Flexibilia. In: Moore R.C (Ed.), *Treatise on Invertebrate Paleontology, Echinodermata*  
1110 *2(2)*. Geological Society of America, Boulder & University of Kansas Press, Lawrence, pp. T759–T812.
- 1111 Moore, R.C. & Plummer, F.B. (1940) Crinoids from the Upper Carboniferous and Permian strata in Texas.  
1112 *University of Texas Publications*, 3495, 9–468.
- 1113 Moore, R.C., Lane, N.G., Strimple, H.L., Sprinkle, J. & Fay, R.O. (1978) Inadunata. In: Moore R.C (Ed.),  
1114 *Treatise on Invertebrate Paleontology, Echinodermata 2(2)*. Geological Society of America, Boulder &  
1115 University of Kansas Press, Lawrence, pp. T520–T759.
- 1116 Nardin, E., Lefebvre, B., David, B. & Mooi, R. (2009) La radiation des échinodermes au Paléozoïque  
1117 inférieur : l'exemple des blastozoaires. *Comptes Rendus Palevol*, 8, 179–188.
- 1118 Nardin, E., Lefebvre, B., Fatka O., Nohejlová, M., Kašička, L., Šinágl, M. & Szabad M. (2017).  
1119 Evolutionary implications of a new transitional blastozoan echinoderm from the mid Cambrian of  
1120 Czech Republic. *Journal of Paleontology*, 91, 672–684.
- 1121 Noailles, F., Lefebvre, B. & Kašička, L. (2014) A probable case of heterochrony in the solutan  
1122 *Dendrocystites* Barrande, 1887 (Echinodermata: Blastozoa) from the Upper Ordovician of the Prague  
1123 Basin (Czech Republic) and a revision of the family Dendrocystitidae Bassler, 1938. *Bulletin of*  
1124 *Geosciences*, 89, 451–476.
- 1125 Öpik, A.A. (1934) *Ristnacrinus*, a new Ordovician crinoid from Estonia. *Tartu Ülikooli Geoloogia-*  
1126 *Instituudi toimetused*, 40, 1–7.
- 1127 Owen, A.W., Bruton, D.L., Bockelie, J.F. & Bockelie, T.G. (1990) The Ordovician successions of the Oslo  
1128 region, Norway. *Norges Geologiske Undersøkelse, Special Publications*, 4, 3–54.
- 1129 Oxley, P. & Kay, M. (1959) Ordovician Chazyan series of Champlain Valley, New York and Vermont, and  
1130 its reefs. *Bulletin of the American Association of Petroleum Geologists*, 43, 817–853.
- 1131 Pander, C.H. (1830) *Beiträge zur Geognosie des Russischen Reiches*. Karl Kray, Saint-Petersburg, 165 pp.
- 1132 Parsley, R.L. (1970) Revision of the North American Pleurocystitidae (Rhombifera - Cystoidea). *Bulletins*  
1133 *of American Paleontology*, 58, 135–213.
- 1134 Parsley, R.L. (1991) Review of selected North American mitrate stylophorans (Homalozoa:  
1135 Echinodermata). *Bulletins of American Paleontology*, 100, 1–57.
- 1136 Parsley, R.L. (1998) Community setting and functional morphology of *Echinosphaerites infaustus*  
1137 (Fistuliporita: Echinodermata) from the Ordovician of Bohemia. *Věstník Ústředního ústavu*  
1138 *geologického*, 73, 253–266.
- 1139 Parsley, R.L. & Caster, K.E. (1965) North American Soluta (Carpoidea, Echinodermata). *Bulletins of*  
1140 *American Paleontology*, 49, 109–174.
- 1141 Paul, C.R.C. (1967) The functional morphology and mode of life of the cystoid *Pleurocystites* E. Billings,  
1142 1854. In: Milot, E. (Ed.), *Echinoderm Biology. Symposium of the Zoological Society of London*, 20,  
1143 105–123.
- 1144 Pisera, A. (1994) Echinoderms from the Mójca Limestone. *Palaeontologia Polonica*, 53, 283–307.
- 1145 Quenstedt, F.A. (1881) *Petrefakten Deutschlands, Part 1, Volume 6. Korallen (Röhren- und Sternkorallen)*.  
1146 Fues, Leipzig, 1093 pp.
- 1147 Rahman, I.A. & Clausen, S. (2009) Re-evaluating the palaeobiology and affinities of the Ctenocystoidea  
1148 (Echinodermata). *Journal of Systematic Palaeontology*, 7, 413–426.



- 1149 Rahman, I.A. & Zamora, S. (2009) The oldest cinctan carpoid (stem-group Echinodermata), and the  
1150 evolution of the water-vascular system. *Zoological Journal of the Linnean Society*, 157, 420–432.
- 1151 Rahman, I.A., Zamora, S. & Geyer, G. (2010) The oldest stylophoran echinoderm: a new *Ceratocystis* from  
1152 the Middle Cambrian of Germany. *Paläontologische Zeitschrift*, 84, 227–237.
- 1153 Rahman, I.A., Waters, J.A., Sumrall, C.D. & Astolfo, A. (2015) Early post-metamorphic, Carboniferous  
1154 blastoid reveals the evolution and development of the digestive system in echinoderms. *Biology Letters*,  
1155 11, 20150776.
- 1156 Raymond, P.E. (1905) The faunas of the Chazy Limestone. *American Journal of Science*, 20, 353–382.
- 1157 Raymond, P.E. (1906) The Chazy Formation and its fauna. *Annals of the Carnegie Museum*, 3, 498–596.
- 1158 Raymond, P.E. (1913) Ordovician of Montreal and Ottawa. *12<sup>th</sup> International Geological Congress*  
1159 *Canada, Guide book*, 3, 137–162.
- 1160 Reed, F.R.C. (1899) The Lower Palaeozoic bedded rocks of County Waterford. *Quarterly Journal of the*  
1161 *Geological Society of London*, 55, 718–772.
- 1162 Regnéll, G. (1956) On *Bolboporites*. *Norsk Geologisk Tidsskrift*, 36, 81.
- 1163 Regnéll, G. (1982) What is *Bolboporites*? In: Lawrence, J.M. (Ed.), *International Echinoderms*  
1164 *Conference, Tampa Bay*. Balkema, Rotterdam, pp. 97.
- 1165 Reich, M. (1999) Ordovizische und silurische Holothurien (Echinodermata). In: Reich, M. (Ed.),  
1166 *Festschrift zum 65. Geburtstag von Ekkehard Herrig*. Greifswalder Geowissenschaftliche Beiträge, 6,  
1167 479–488.
- 1168 Reich, M. (2001) *Linguaserra?* (Echinodermata: Ophiocistoidea) aus dem Ordovizium Baltoskandiens.  
1169 *Greifswalder Geowissenschaftliche Beiträge*, 9, 33–35.
- 1170 Reich, M. (2010) The oldest synallactid sea cucumber (Echinodermata: Holothuroidea: Aspidochirotida).  
1171 *Paläontologische Zeitschrift*, 84, 541–546.
- 1172 Reich, M. & Smith, A.B. (2009) Origins and biomechanical evolution of teeth in echinoids and their  
1173 relatives. *Palaeontology*, 52, 1149–1168.
- 1174 Roemer, C.F. (1854) Beiträge zur geologischen Kenntnis des nordwestlichen Harzgebirges,  
1175 *Palaeontographica*, 3, 1–67.
- 1176 Roemer, C.F. (1885) *Lethaea erratica* oder Aufzählung und Beschreibung der in der norddeutschen Ebene  
1177 vorkommenden Diluvial-Geschiebe nordischer Sedimentärgesteine. *Paläontologische Abhandlungen*, 2,  
1178 250–420.
- 1179 Rouault, M. (1851) Mémoire sur le terrain paléozoïque des environs de Rennes. *Bulletin de la Société*  
1180 *géologique de France*, 8, 358–399.
- 1181 Rozhnov, S.V. (2002) Morphogenesis and evolution of crinoids and other pelmatozoan echinoderms in the  
1182 Early Paleozoic. *Paleontological Journal*, 36, 525–674.
- 1183 Rozhnov, S.V. (2005) Echinoderms. In: Dronov, A., Tolmacheva, T., Raevskaya, E. & Nestell, M. (Eds.),  
1184 *Cambrian and Ordovician of St. Petersburg area. Guidebook of the pre-conference field trip*. St.  
1185 Petersburg State University, Saint-Petersburg, pp. 23–26.
- 1186 Rozhnov, S.V. (2009). New data on Ordovician eocrinoids and paracrinoids of the Baltic Region.  
1187 *Geophysical Research Abstracts*, 11, EGU2009-3683-1.
- 1188 Rozhnov, S.V. & Kushlina, V.B. (1994a) A new interpretation of *Bolboporites* (Echinodermata,  
1189 ?Eocrinoidea). *Paleontological Journal*, 28, 71–80.
- 1190 Rozhnov, S.V. & Kushlina, V.B. (1994b) Interpretation of new data on *Bolboporites* Pander, 1830  
1191 (Echinodermata; Ordovician). In: David, B., Guille, A., Féral, J.P. & Roux, M. (Eds.), *Echinoderms*  
1192 *through Time*. Balkema, Rotterdam, pp. 179–180.
- 1193 Ruedemann, R. (1901) Trenton conglomerate of Rysedorph Hill, Rensselaer County, New York and its  
1194 fauna. *New York State Museum Bulletin*, 49, 1–114.
- 1195 Ruta, M. (1999) A new stylophoran echinoderm, *Juliaecarpus milnerorum*, from the Late Ordovician  
1196 Upper Ktaoua Formation of Morocco. *Bulletin of the Natural History Museum, London (Geology)*, 55,  
1197 47–79.

- 1198 Ruta, M. & Bartels, C. (1998) A redescription of the anomalocystitid mitrate *Rhenocystis latipedunculata*  
1199 from the Lower Devonian of Germany. *Palaeontology*, 41, 771–806.
- 1200 Schmidt, H. (1951) Whitehouse's Ur-Echinodermen aus dem Cambrium Australiens. *Paläontologische*  
1201 *Zeitschrift*, 24, 142–145.
- 1202 Seilacher, A. & MacClintock, C. (2005) Crinoid anchoring strategies for soft-bottom dwelling. *Palaios*, 20,  
1203 224–240.
- 1204 Shaw, F.C. & Bolton, T.E. (2011) Ordovician trilobites from the Romaine and Mingan formations  
1205 (Ibexian–late Whiterockian), Mingan Islands, Quebec. *Journal of Paleontology*, 85, 406–441.
- 1206 Smith, A.B. (1980a) Stereom microstructure of the echinoid test. *Special Papers in Palaeontology*, 25, 1–  
1207 81.
- 1208 Smith, A.B. (1980b) The structure and arrangement of echinoid tubercles. *Philosophical Transactions of*  
1209 *the Royal Society, B*, 289, 1–46.
- 1210 Smith, A.B. (1982) The affinities of the Middle Cambrian Haplozoa (Echinodermata). *Alcheringa*, 6, 93–  
1211 99.
- 1212 Smith, A.B. (1988) Patterns of diversification and extinction in Early Palaeozoic echinoderms.  
1213 *Palaeontology*, 31, 799–828.
- 1214 Smith, A.B. & Savill, J.J. (2001) *Bromidechinus*, a new Ordovician echinozoan (Echinodermata), and its  
1215 bearing on the early history of echinoids. *Transactions of the Royal Society of Edinburgh (Earth*  
1216 *Sciences)*, 92, 137–147.
- 1217 Smith, A.B. & Zamora, S. (2009) Rooting phylogenies of problematic fossil taxa; a case study using  
1218 cinctans (stem-group echinoderms). *Palaeontology*, 52, 803–821.
- 1219 Spencer, W.K. & Wright, C.W. (1966) Asterozoans. In: Moore R.C (Ed.), *Treatise on Invertebrate*  
1220 *Paleontology, Echinodermata 3(1)*. Geological Society of America, Boulder & University of Kansas  
1221 Press, Lawrence, pp. U4–U107.
- 1222 Spjeldnaes, N. & Nitecki, M.H. (1990) *Coelosphaeridium*, an Ordovician alga from Norway. *Institutt for*  
1223 *Geologi Universitetet I Oslo, Intern Skriftserie*, 59, 1–53.
- 1224 Springer, F. (1926) Unusual forms of fossil crinoids. *Proceedings of the United States National Museum*,  
1225 67, 1–137.
- 1226 Sprinkle, J. (1973) Morphology and evolution of blastozoan echinoderms. *Harvard University Museum of*  
1227 *Comparative Zoology, Special Publication*, 1–283.
- 1228 Sprinkle, J. & Guensburg, T.E. (2001) Growing a stalked echinoderm within the Extraxial-Axial Theory.  
1229 In: Barker, F.K. (Ed.), *Echinoderms 2000*. Swets & Zeitlinger, Lisse, pp. 59–65.
- 1230 Stanton, R.J., Jr., Lambert, L.L., Webb, G.E. & Lustig, L.D. (2016) *Chaetetes* morphology, environment,  
1231 and taxonomy. *Facies*, 62:29, 1–21.
- 1232 Strimple, H.L. (1961) Late Desmoinesian crinoid faunule from Oklahoma. *Bulletin of the Oklahoma*  
1233 *Geological Survey*, 93, 1–189.
- 1234 Strimple, H.L. & Watkins, W.T. (1969) Carboniferous crinoids of Texas with stratigraphic implications.  
1235 *Palaeontographica Americana*, 6, 41–275.
- 1236 Sumrall, C.D., Sprinkle, J. & Guensburg, T.E. (1997) Systematics and paleoecology of late Cambrian  
1237 echinoderms from the western United States. *Journal of Paleontology*, 71, 1091–1109.
- 1238 Sutton, M.D., Briggs, D.E.G., Siveter, D.J., Siveter, D.J. & Gladwell, D.J. (2005) A starfish with three-  
1239 dimensionally preserved soft parts from the Silurian of England. *Proceedings of the Royal Society B*,  
1240 272, 1001–1006.
- 1241 Termier, H. & Termier, G. (1950) Contribution à l'étude des faunes paléozoïques de l'Algérie. *Bulletin du*  
1242 *Service de la Carte Géologique de l'Algérie*, 1–83.
- 1243 Thoral, M. (1935) *Contribution à l'Etude Paléontologique de l'Ordovicien Inférieur de la Montagne Noire*  
1244 *et Révision Sommaire de la Faune Cambrienne de la Montagne Noire*. Imprimerie de la Charité,  
1245 Montpellier, 362 pp.
- 1246 Tinn, O. & Ainsaar, L. (2014) Asterozoan pedicellariae and ossicles revealed from the Middle Ordovician  
1247 of Baltica. *Acta Palaeontologica Polonica*, 59, 353–358.

- 1248 Twenhofel, W.H. (1938) Geology and paleontology of the Mingan Islands, Quebec. *Geological Society of*  
1249 *America, Special Paper*, 11, 1–132.
- 1250 Ubaghs, G. (1961) Un échinoderme nouveau de la classe des carpoïdes dans l'Ordovicien inférieur du  
1251 département de l'Hérault (France). *Comptes-Rendus de l'Académie des Sciences, Paris*, 253, 2565–  
1252 2567.
- 1253 Ubaghs, G. (1963) *Rhopalocystis destombesi* n.g., n.sp., éocrinoïde de l'Ordovicien inférieur (Trémadocien  
1254 supérieur) du Sud marocain. *Notes du Service géologique du Maroc*, 23, 25–44.
- 1255 Ubaghs, G. (1968a) Stylophora. In: Moore, R.C (Ed.), *Treatise on Invertebrate Paleontology,*  
1256 *Echinodermata 1(2)*. Geological Society of America, Boulder & University of Kansas Press, Lawrence,  
1257 pp. S495–S565.
- 1258 Ubaghs, G. (1968b) *Cymbionites* and *Peridionites* - unclassified Middle Cambrian echinoderms. In: Moore,  
1259 R.C (Ed.), *Treatise on Invertebrate Paleontology, Echinodermata 1(2)*. Geological Society of America,  
1260 Boulder & University of Kansas Press, Lawrence, pp. S634–S637.
- 1261 Ubaghs, G. (1969) *Aethocrinus moorei* Ubaghs, n. gen., n. sp., le plus ancien crinoïde dicyclique connu.  
1262 *University of Kansas Paleontological Contributions*, 38, 1–25.
- 1263 Ubaghs, G. (1970) *Les Echinodermes "Carpoïdes" de l'Ordovicien Inférieur de la Montagne Noire*  
1264 *(France)*. Editions du CNRS, Cahiers de Paléontologie, Paris, 110 pp.
- 1265 Ubaghs, G. (1972) Le genre *Balantiocystis* Chauvel (Echinodermata, Eocrinoidea) dans l'Ordovicien  
1266 inférieur de la Montagne Noire (France). *Annales de Paléontologie*, 58, 3–27.
- 1267 Ubaghs, G. (1978a) Skeletal morphology of fossil crinoids. In: Moore R.C (Ed.), *Treatise on Invertebrate*  
1268 *Paleontology, Echinodermata 2(1)*. Geological Society of America, Boulder & University of Kansas  
1269 Press, Lawrence, pp. T58–T216.
- 1270 Ubaghs, G. (1978b) Camerata. In: Moore R.C (Ed.), *Treatise on Invertebrate Paleontology, Echinodermata*  
1271 *2(1)*. Geological Society of America, Boulder & University of Kansas Press, Lawrence, pp. T408–T518.
- 1272 Ubaghs, G. (1981) Réflexions sur la nature et la fonction de l'appendice articulé des "carpoïdes"  
1273 Stylophora (Echinodermata). *Annales de Paléontologie*, 67, 33–48.
- 1274 Ubaghs, G. (1983) Echinodermata. Notes sur les Échinodermes de l'Ordovicien Inférieur de la Montagne  
1275 Noire (France). In: Courtessole, R., Marek, L., Pillet, J., Ubaghs, G. & Vizcaïno, D. (Eds.), *Calymena,*  
1276 *Echinodermata et Hyolitha de l'Ordovicien de la Montagne Noire (France Méridionale)*. Société  
1277 d'Etudes Scientifiques de l'Aude, Carcassonne, p. 33–35.
- 1278 Wanner, J. (1920) Ueber einige palaeozoische Seeigelstacheln (*Timorocidaris* gen. nov. und *Bolboporites*  
1279 Pander). *Proceedings of the Koninklijke Nederlandse Akademie van Wetenschappen*, 22, 696–712.
- 1280 Wanner, J. (1924) Die permischen Blastoiden von Timor. *Jaarboek van het mijnwezen in Nederlands Oost-*  
1281 *Indie*, 51, 163–233.
- 1282 Webster, G.D. & Kues, B.S. (2006) Pennsylvanian crinoids of New Mexico. *New Mexico Geology*, 28, 3–  
1283 39.
- 1284 White, T.G. (1896) Geology of Essex and Willsboro townships, Essex County, New York. *Transactions of*  
1285 *the New York Academy of Sciences*, 13, 214–233.
- 1286 Whitehouse, F.W. (1941) The Cambrian faunas of north-eastern Australia. Part 4: Early Cambrian  
1287 echinoderms similar to the larval stages of recent forms. *Memoirs of the Queensland Museum*, 12, 1–28.
- 1288 Wyse Jackson, P.N., Buttler, C.J. & Key, M.M. (2002) Palaeoenvironmental interpretation of the Tramore  
1289 Limestone Formation (Llandeilo, Ordovician) based on bryozoan colony form. In: Wyse Jackson, P.N.,  
1290 Buttler, C.J. & Spencer Jones, M.E. (Eds.), *Bryozoan Studies 2001*. Swets & Zeitlinger, Lisse, pp. 359–  
1291 365.
- 1292 Yakovlev, N.N. (1921). *Bolboporites*, its structure and affinity to the Hydrozoa. *Annals of the Russian*  
1293 *Paleontological Association*, 3, 1–10 [in Russian, with an abstract in English]
- 1294 Yeltysheva, R.S. (1955) *Bolboporites*. *Voprosy Paleontologii*, 2, 136–147 [in Russian].
- 1295 Zamora, S., Alvaro, J.J. & Vizcaïno, D. (2009) Pelmatozoan echinoderms from the Cambrian-Ordovician  
1296 of the Iberian Chains (NE Spain): early diversification of anchoring strategies. *Swiss Journal of*  
1297 *Geosciences*, 102, 43–55.

1298 Zamora, S., Lefebvre, B., Alvaro, J.J., Clausen, S., Elicki, O., Fatka, O., Jell, P., Kouchinsky, A., Lin, J.P.,  
1299 Nardin, E., Parsley, R.L., Rozhnov, S.V., Sprinkle, J., Sumrall, C.D., Vizcaino, D. & Smith, A.B.  
1300 (2013) Cambrian echinoderm diversity and palaeobiogeography. *In: Harper, D.A.T & Servais, T.*  
1301 *(Eds.), Early Palaeozoic Biogeography and Palaeogeography. Geological Society, London, Memoirs,*  
1302 *38, 157–171.*

1303 Zittel, K.A. von (1879) *Handbuch der Paläontologie. 1. Band, 1. Protozoa, Coelenterata, Echinodermata*  
1304 *und Molluscoidea.* Oldenburg, München & Leipzig, 765 pp.

1306

1307

1308

1309

1310

### 1311 **Figure Captions**

1312

1313 **FIGURE 1.** External morphology of *Bolboporites uncinatus* Pander, 1830, Middle  
1314 Ordovician (Dapingian), Saint-Petersburg area, Russia; redrawn and modified from Rozhnov  
1315 & Kushlina (1994a, fig. 3b) and Kushlina (1995, pl. 5 fig. 1b). A: Base of the cone, in front  
1316 view, showing the two adjoining depressed areas (lunules), and the small orifice  
1317 corresponding to the outlet of the longitudinal internal canal. B: Lateral view, showing the  
1318 typical honeycomb ornamentation on lateral sides of the cone.

1319

1320 **FIGURE 2.** Fourier transform infrared (FT-IR) spectroscopy made on transverse sections of  
1321 *Bolboporites mitralis* Pander, 1830, included in LR white resin; UCBL-FSL 712510, Middle  
1322 Ordovician (Dapingian), Saint-Petersburg area, Russia. A: Location of FTIR analyses. B: IF  
1323 spectrum of LR white resin (control spectrum). C, G: IF spectra of sampling points located on  
1324 the external margin of the specimen (calcite). D-F: IF spectra of sampling points within the  
1325 specimen (calcite). Peak values indicated in  $\text{cm}^{-1}$ .

1326

1327 **FIGURE 3.** Thin section views of *Bolboporites mitralis* Pander, 1830 (Middle Ordovician  
1328 (Dapingian), Saint-Petersburg area, Russia; UCBL-FSL 712510) included in the surrounding  
1329 sedimentary rock (ss) which is a packstone-wackestone with bioclasts and glauconite grains.  
1330 A: Plane-polarized optical light, showing the conjugated cleavage planes (cp) crosscutting the  
1331 whole cone. B: Cross-polarized optical light, showing total extinction of the cone. C: Close up

1332 view of A and B (plane polarized light) revealing the tenuous dark-brown patches aligned  
1333 along cleavage planes, forming a stereom-like structure.

1334

1335 **FIGURE 4.** EBSD mapping of *Bolboporites mitralis* Pander, 1830; Middle Ordovician  
1336 (Dapingian), Saint-Petersburg area, sample UCLB-FSL 712510, cross section, perpendicular  
1337 to the cone axis. A: Periphery of the sample observed by SEM. B: corresponding EBSD map,  
1338 showing the size heterogeneity of the crystals around the monocrystalline structure; the box  
1339 on the down right corner gives the color code for crystallographic axes. C: another peripheral  
1340 zone, at higher magnification. D: corresponding EBSD map. E: central zone of *B. mitralis*  
1341 visualized by SEM. F and G: two EBSD maps of two areas of the central zone (E) 4 mm  
1342 apart. Although the structure is fully monocrystalline on the whole cross-section (no grain  
1343 limit detectable), a slight variation of the colour indicates a tiny crystallographic  
1344 disorientation ( $< 4^\circ$ ).

1345

1346 **FIGURE 5.** Internal structures of *Bolboporites mitralis* Pander, 1830; Middle Ordovician  
1347 (Dapingian), Saint-Petersburg area, Russia. A-C: Cathodoluminescence view of sectioned  
1348 *Bolboporites mitralis* Pander, 1830; Middle Ordovician (Dapingian), Saint-Petersburg area,  
1349 Russia. A: Longitudinal section through specimen UCBL-FSL 712508, with several randomly  
1350 distributed *Trypanites*-like borings (bor) through the body wall. B-C: Cross section through  
1351 specimen UCBL-FSL 712510, showing evidence of narrow longitudinal axial canal (int.  
1352 canal). B: General view of the sectioned specimen. C: Detail showing the central internal  
1353 canal filled with a syntaxial blocky calcite cement (sbc). The surrounding skeleton reveals a  
1354 stereom-like structure with aligned luminescent inclusions; specimen UCBL-FSL 712510 D:  
1355 This SEM view shows the opening part of a tubular boring crosscutting the stereom-like  
1356 microstructure of a *Bolboporites* cone (UCBL-FSL 712508). Note this stereom-like  
1357 microstructure is highly cemented near the walls of the boring and at the periphery of the  
1358 cone, whereas micropores (mp) are presents in the more internal parts. This boring is partially  
1359 filled with a bioclastic and glauconitic packstone (gp) that also surround the cone. More  
1360 internal parts of the boring are cemented by dolomite rhombs (dol) and by a syntaxial blocky  
1361 calcite cement (sbc).

1362

1363 **FIGURE 6.** CT-scan imagery of *Bolboporites mitralis* Pander, 1830; UCBL-FSL 712509  
1364 Middle Ordovician (Dapingian), Saint-Petersburg area, Russia. A: Virtual cross section  
1365 showing diffuse peripheral rim, made of denser (less porous) stereom than central part of the

1366 cone, as also shown on SEM imagery (Fig 5B). This view is reminiscent, in part, to a section  
1367 through a cidaroid spine (see, e.g., Donovan 2018). Lateral honeycomb cells appear clearly on  
1368 external margin of peripheral rim. B: Three-dimensional reconstruction of the specimen, with  
1369 line indicating location of cross section in A.

1370

1371 **FIGURE 7.** External aspect and morphological disparity of *Bolboporites*; all specimens from  
1372 same locality and level, Upper Ordovician (Sandbian), Skien-Langesund area, Norway. A:  
1373 *Bolboporites* sp., lateral side of the cone showing honeycomb ornamentation, and almost flat  
1374 base of the cone; PMO 116887. B: *Bolboporites elongatus* Kushlina, 1995, narrow cone in  
1375 lateral view, with gently convex base; PMO 218238. C-D: *Bolboporites* cf. *mitralis* Pander,  
1376 1830; PMO 218249. C: Wide cone in lateral aspect, with convex base. D: Basal surface with  
1377 two lunules in almost central position, and small orifice at their junction.

1378

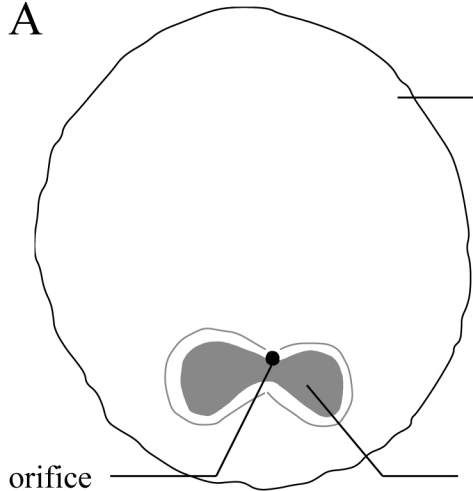
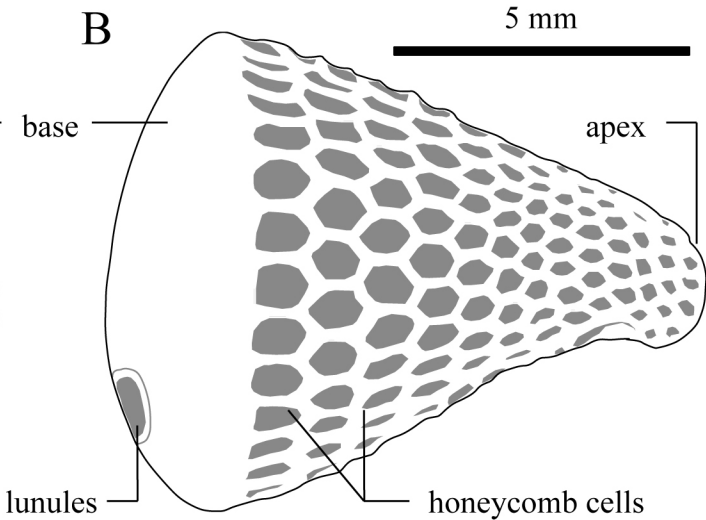
1379 **FIGURE 8.** External morphology of *Bolboporites mitralis* Pander, 1830; Middle Ordovician  
1380 (Dapingian), Saint-Petersburg area, Russia. A: Cells forming honeycomb ornamentation on  
1381 lateral sides of the cone; SEM view of specimen UCBL-FSL 713254. B: Lunules and  
1382 associated small orifice, on the base of the cone; SEM view of specimen UCBL-FSL 713250.  
1383 Note also the well-preserved stereom-like microstructure that appears on the wall of these  
1384 lunules.

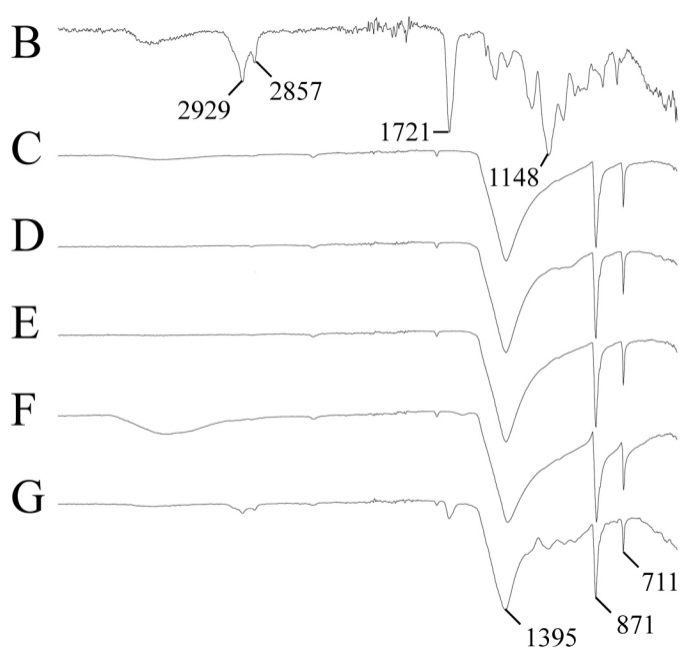
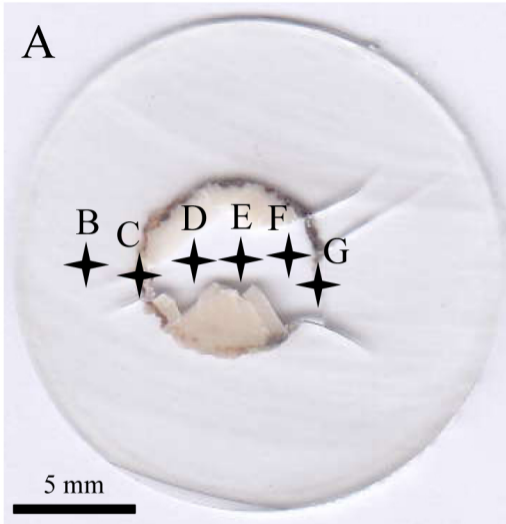
1385

1386 **FIGURE 9.** Aboral tubercles of the Recent oreasterid asteroid *Pentaceraster mammilatus*  
1387 (Audouin, 1826). A: Extracted tubercle in lateral view, with its lateral walls covered by thick,  
1388 polyplated, granulose aboral membrane; specimen UCBL.2017.01.44. B-E: Specimen  
1389 UCBL.2017.01.47. B: Extracted tubercle in oblique view, with its basal surface showing  
1390 several diverging branches, connecting it with surrounding aboral plates. C: Cross-section of  
1391 extraction site of tubercle shown in (B), on the aboral surface, showing complex articulation  
1392 of tubercle-bearing plate with surrounding aboral skeletal elements. D: General view of aboral  
1393 surface. E: Close-up of aboral surface showing area of extraction of the spiny tubercle.

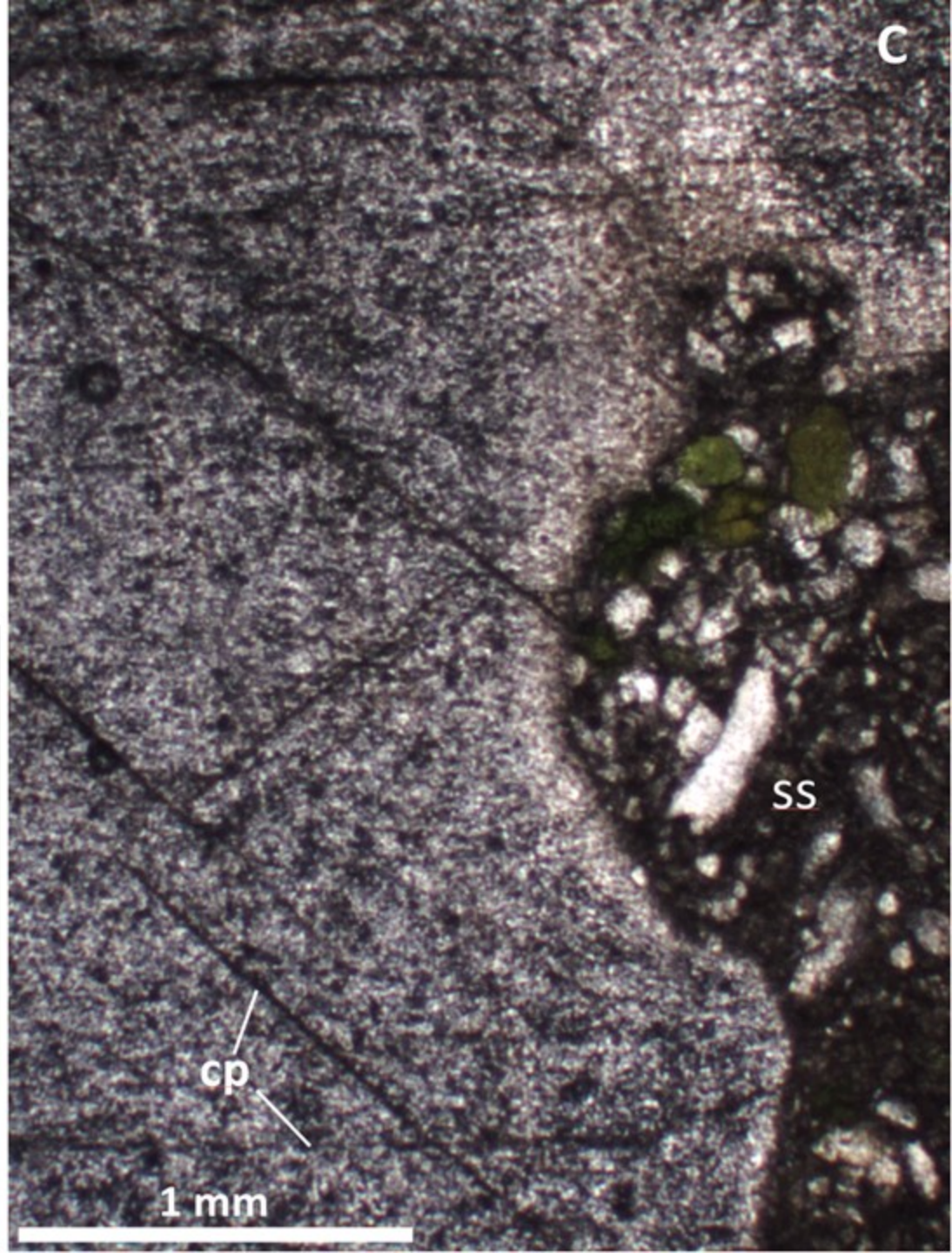
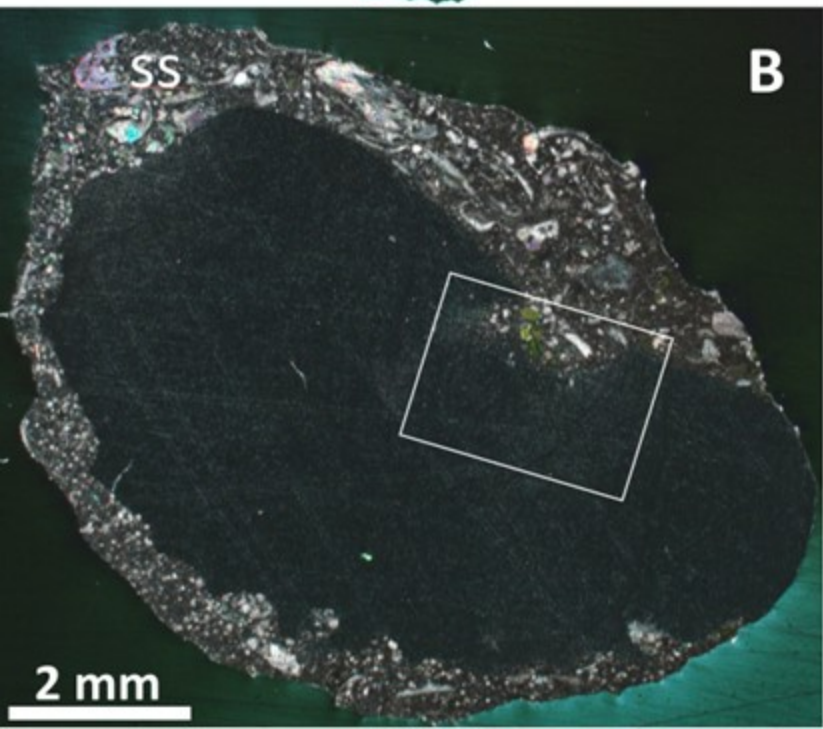
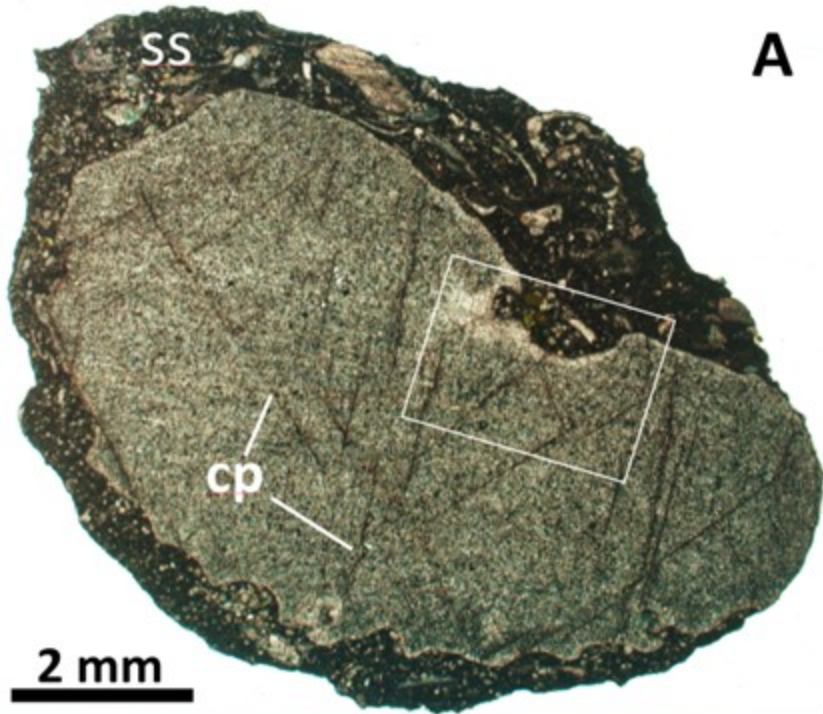
1394

1395

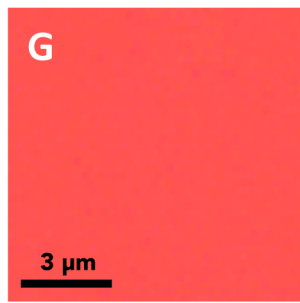
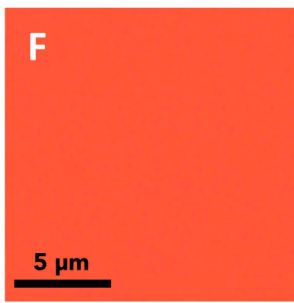
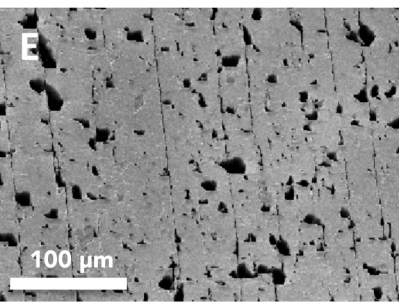
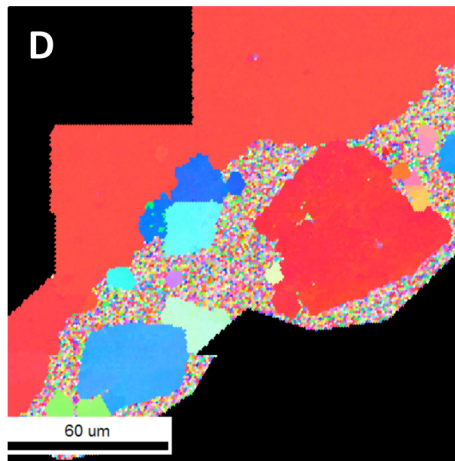
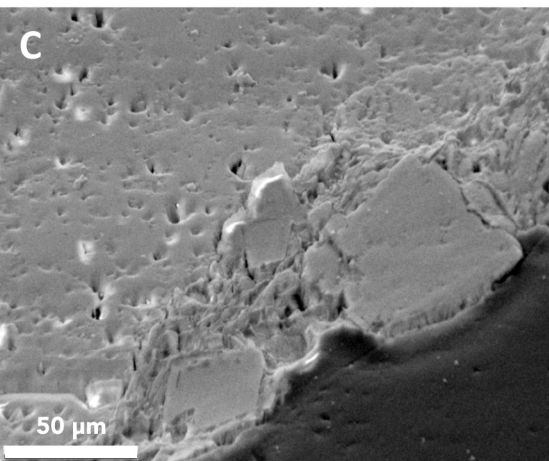
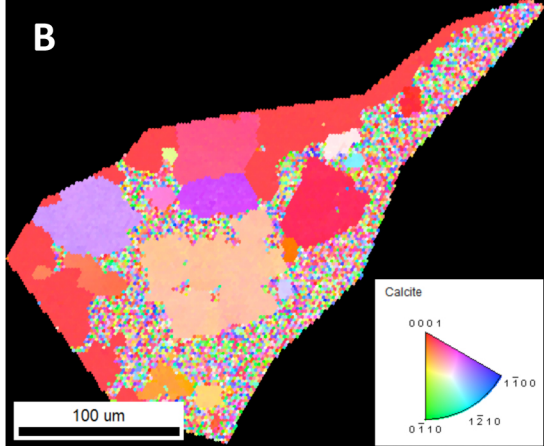
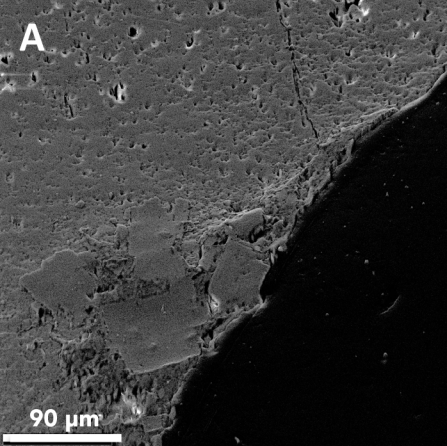
**A****B**

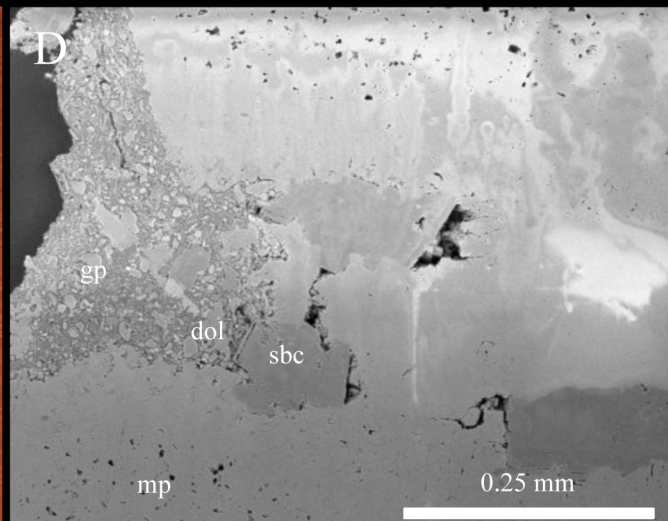
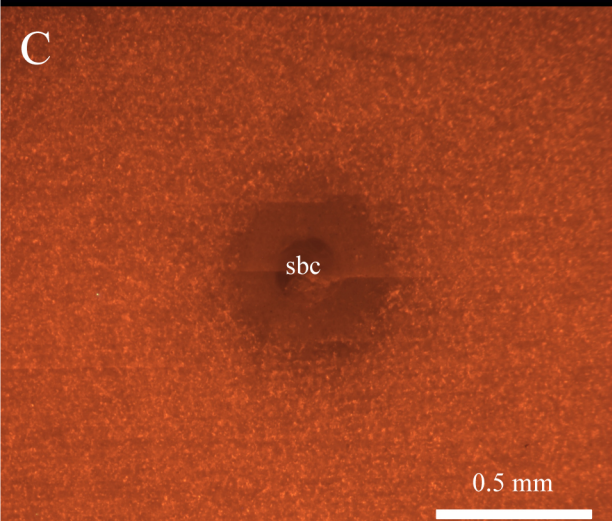
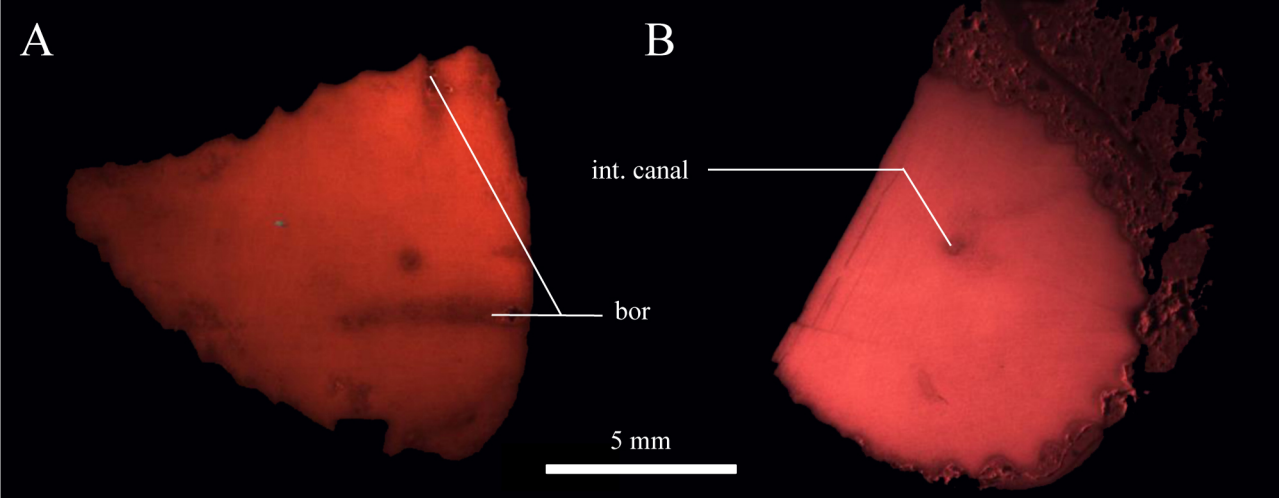


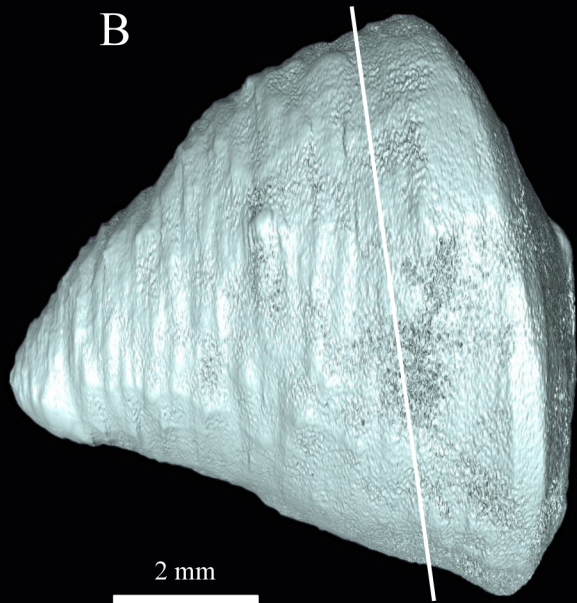
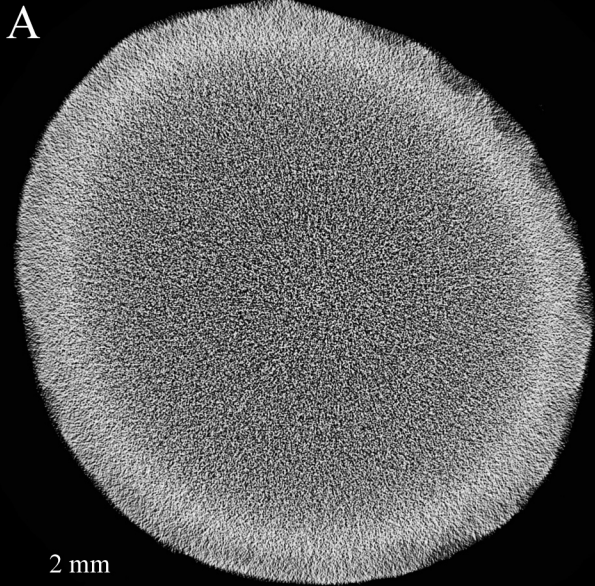


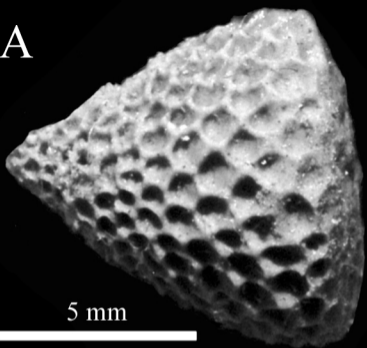
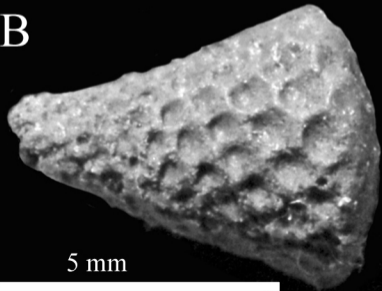










**A****B****C****D**



